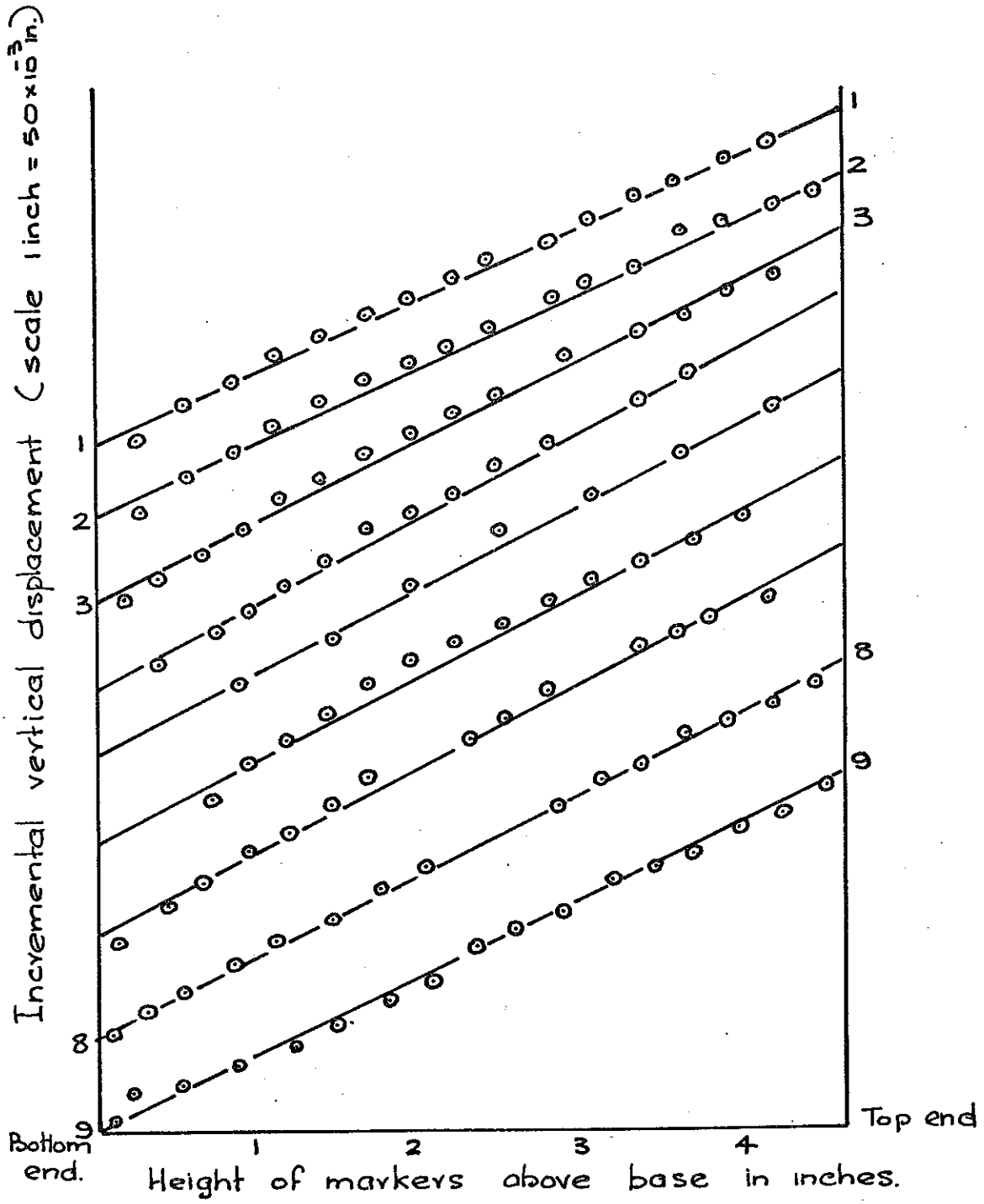

3.17 (a) Incremental vertical displacement of markers plotted against height of markers above base for nine vertical columns in plane 1 of specimen OC during isotropic consolidation

(stress increment 30 to 50 psi)

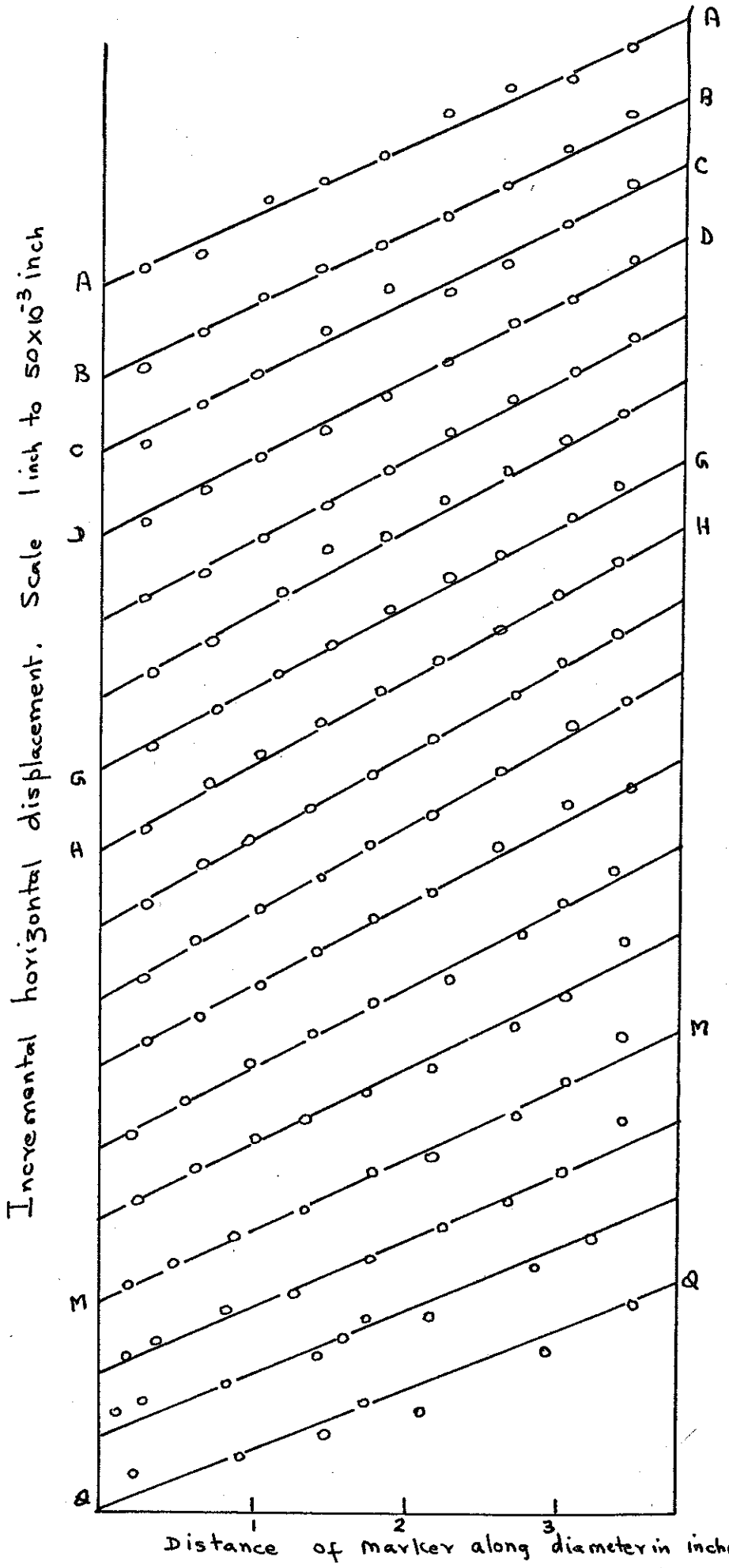

Fig. 3.17 (b). Incremental horizontal displacement of markers plotted against their distances along the diameter for seventeen horizontal rows in plane I during isotropic consolidation.

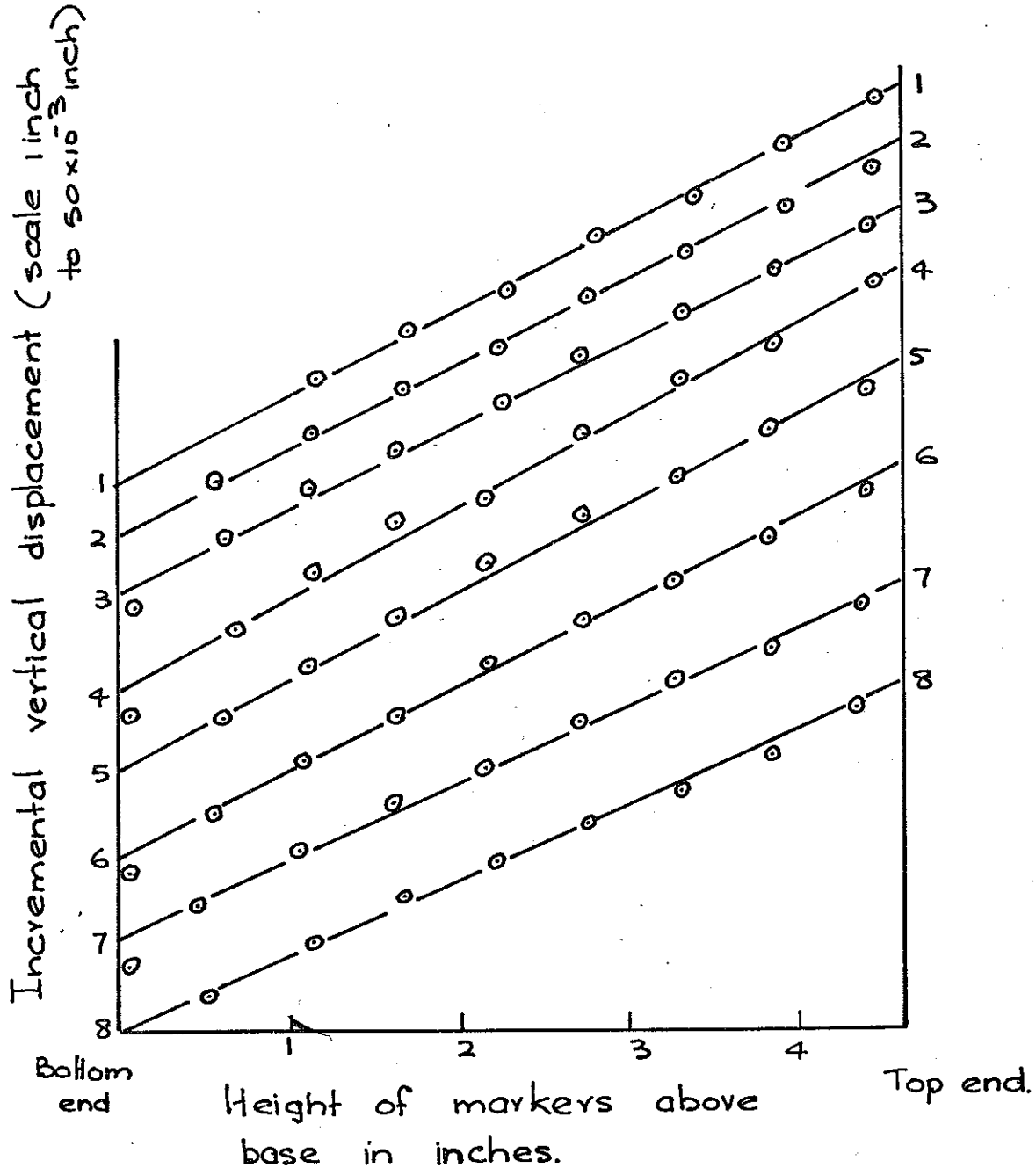

Fig. 3.17 (c) Incremental vertical displacement of lead markers plotted against their heights above base, for eight vertical columns in plane 2 of sample OC during isotropic consolidation.

(stress increment 30 - 50 psi)

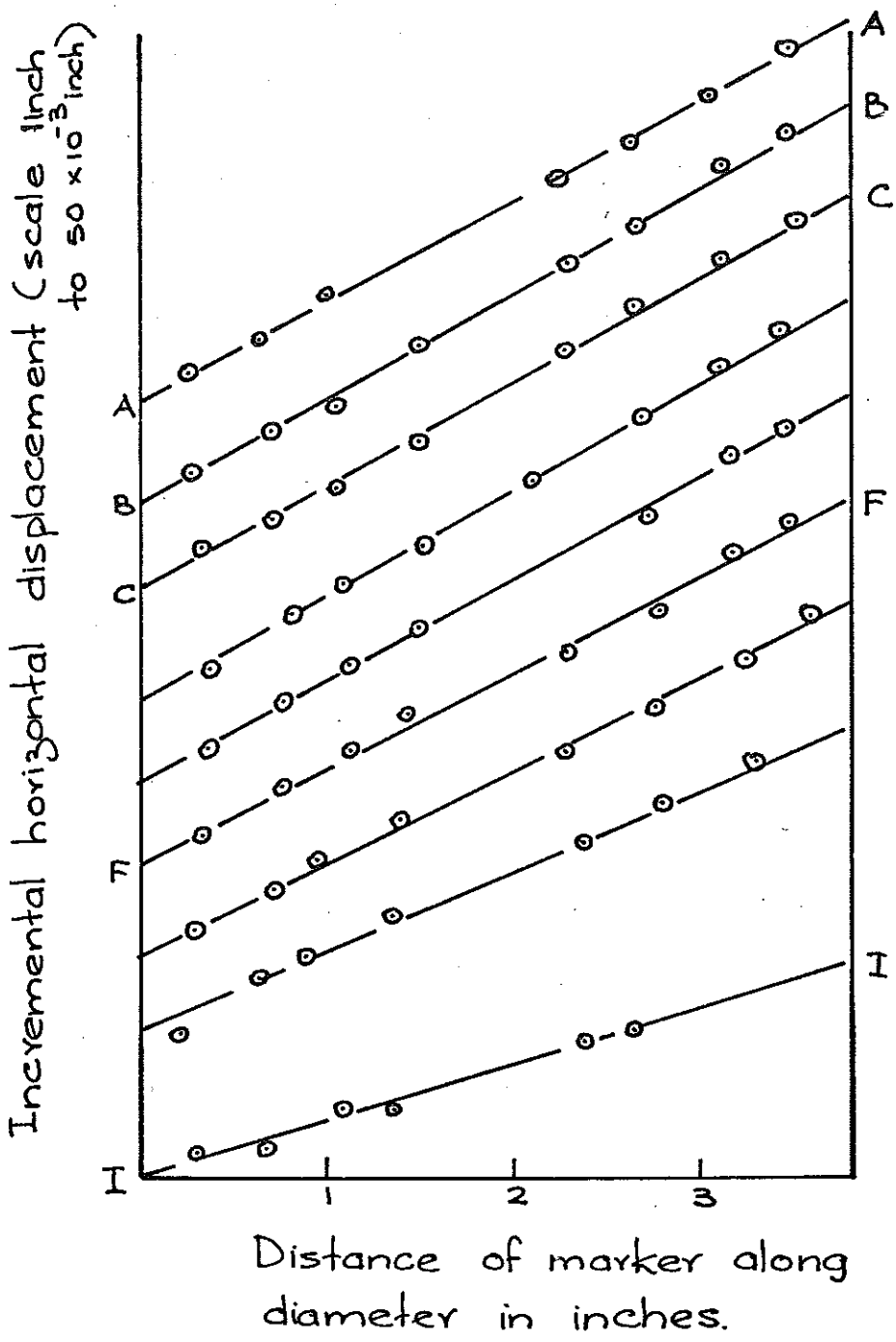

Fig. 3.17 (d) Incremental horizontal displacement of markers plotted against their distances along the diameter for nine horizontal rows in plane 2 of sample OC during isotropic consolidation.

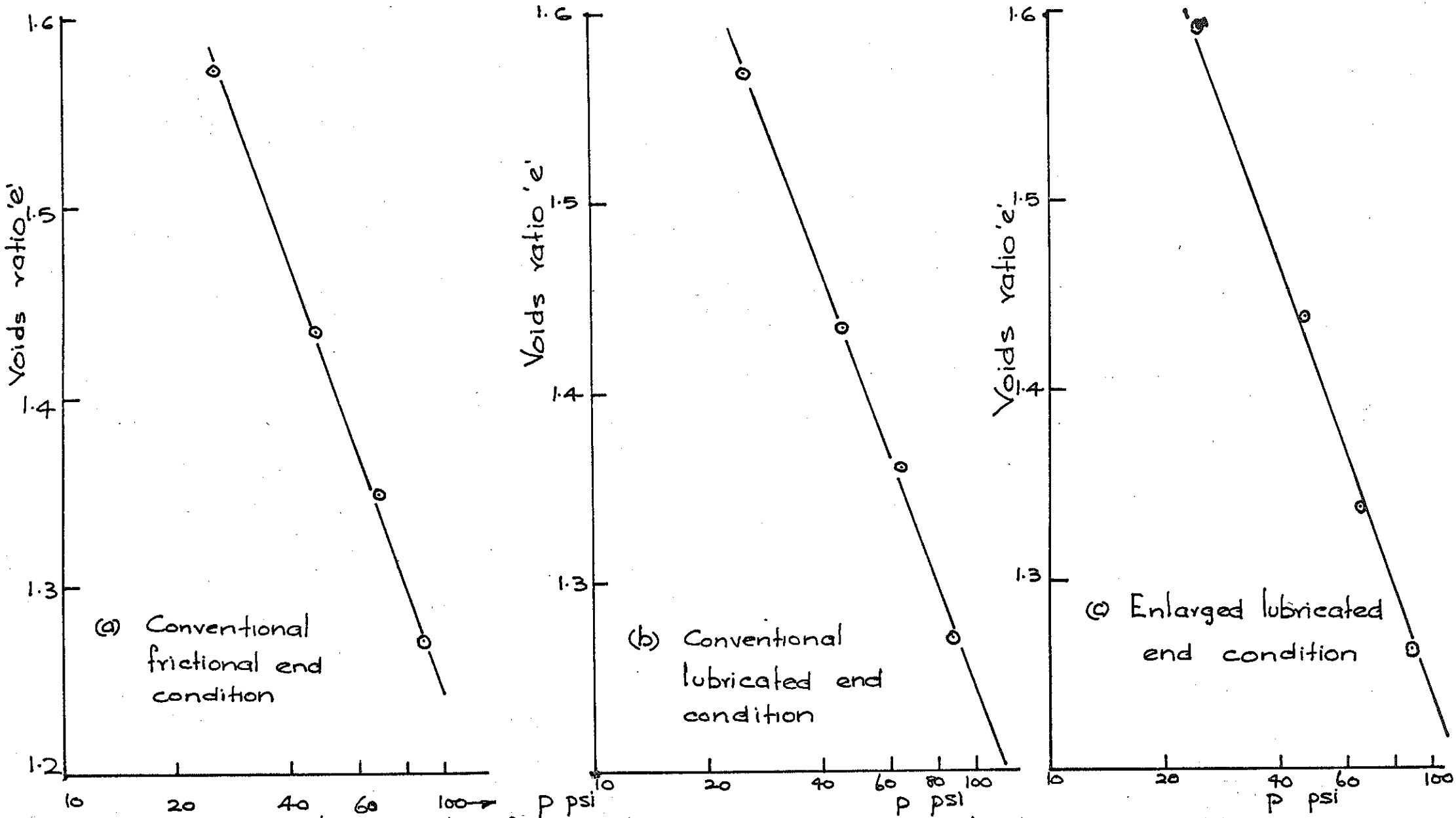

Fig. 3.18. 'e' Vs. log p plots for isotropic consolidation tests.

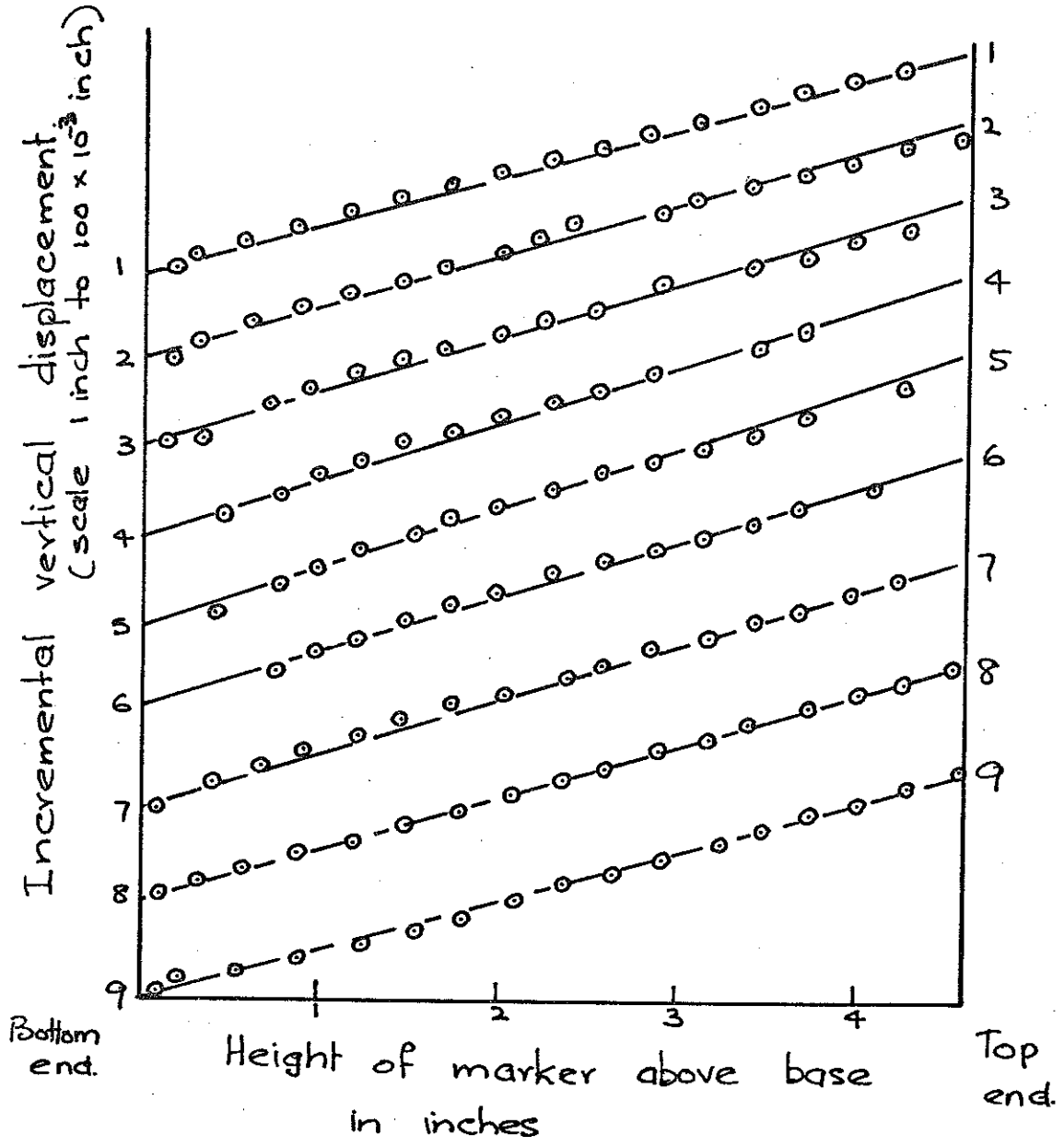

Fig. 3.19@ Incremental vertical displacements of lead markers plotted against their heights above base for nine vertical columns in plane 1 of sample OC during isotropic swelling.

(Reduction of isotropic stress from 60 to 5 psi.

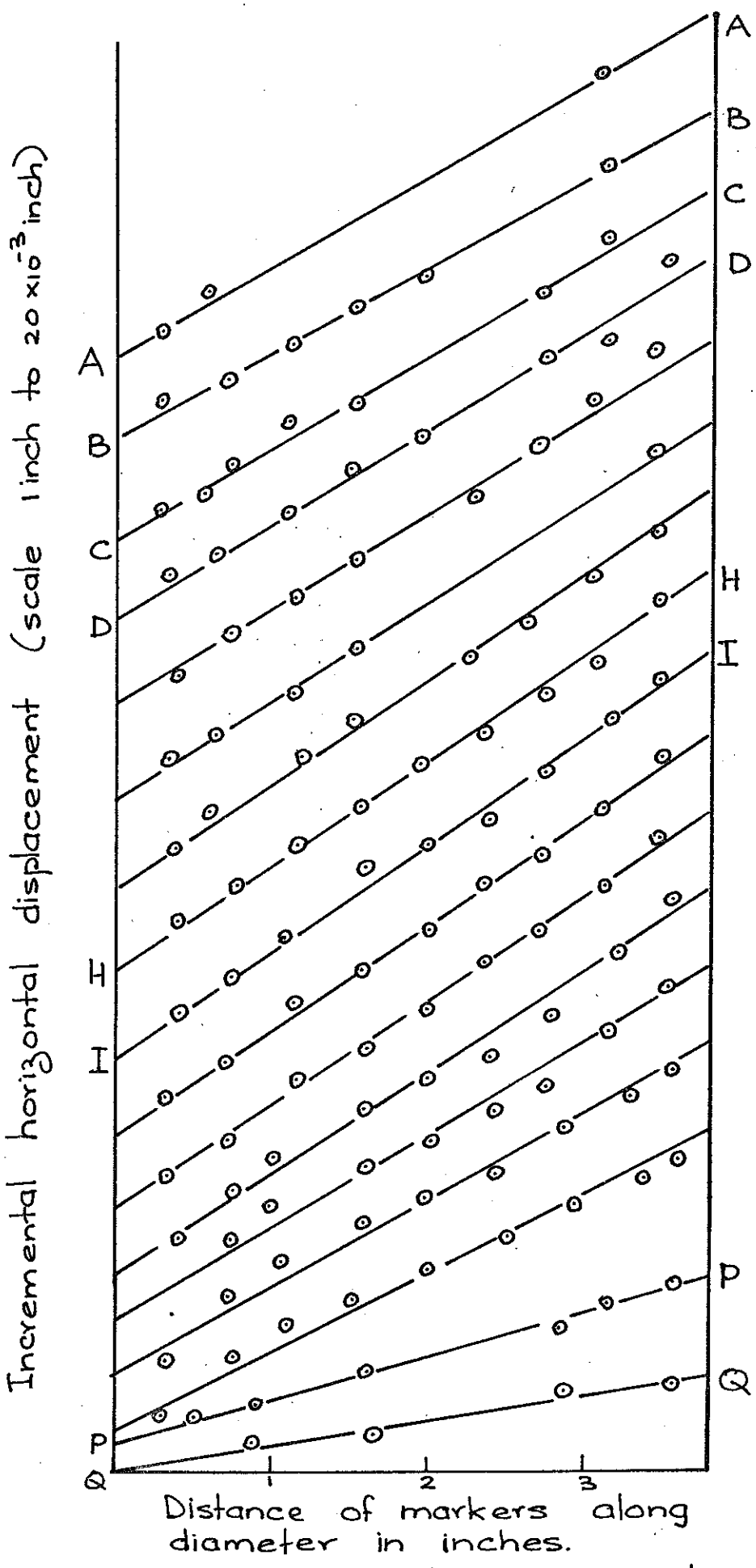

Fig. 3.19(b) Incremental horizontal displacements of lead markers plotted against their distances along diameter for 17 horizontal rows in plane I of sample OC during isotropic swelling.

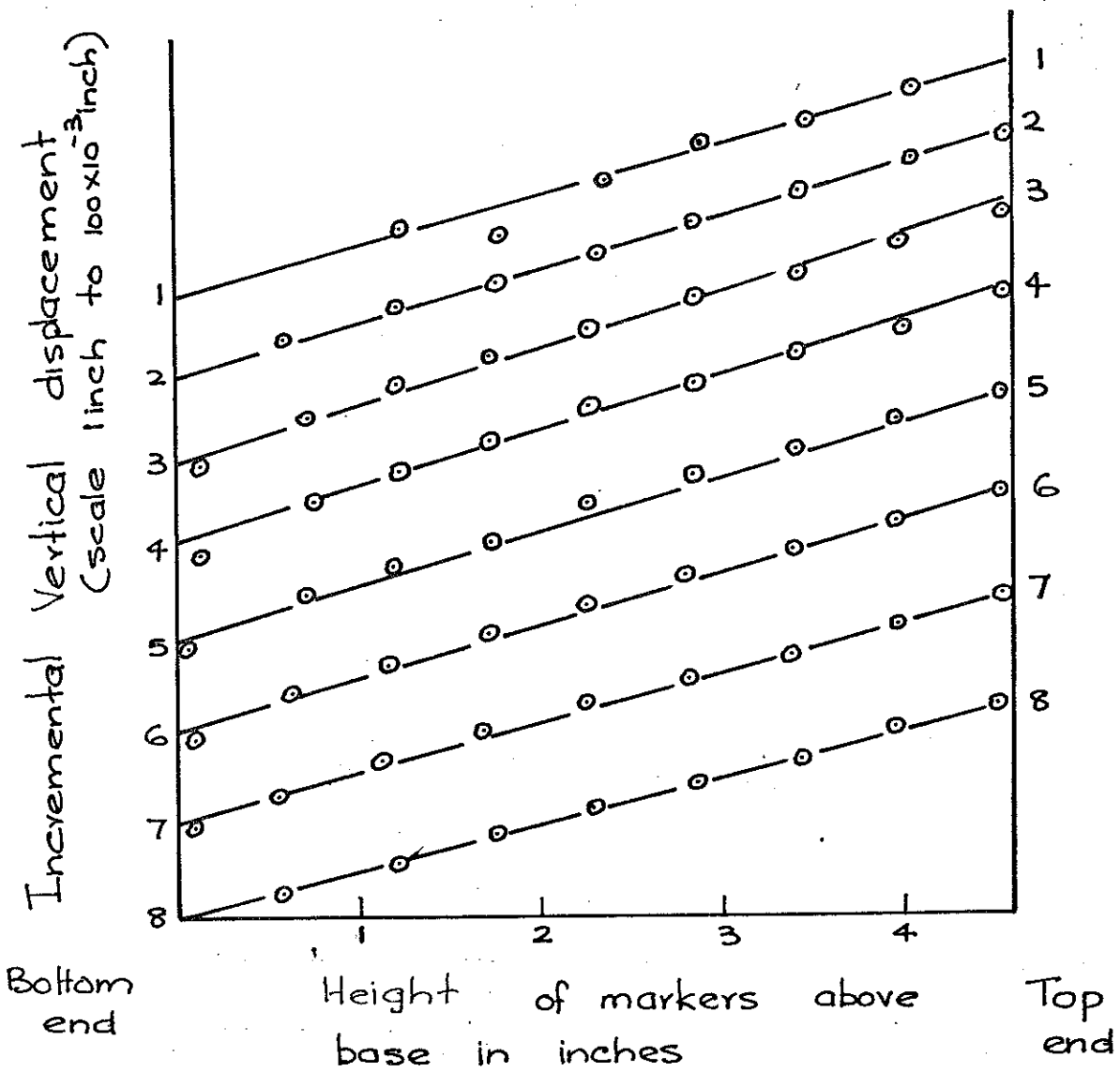

3.20 (a) Incremental vertical displacements of lead markers plotted plotted against their heights above base for eight vertical columns in plane 1 of sample OC during isotropic swelling.

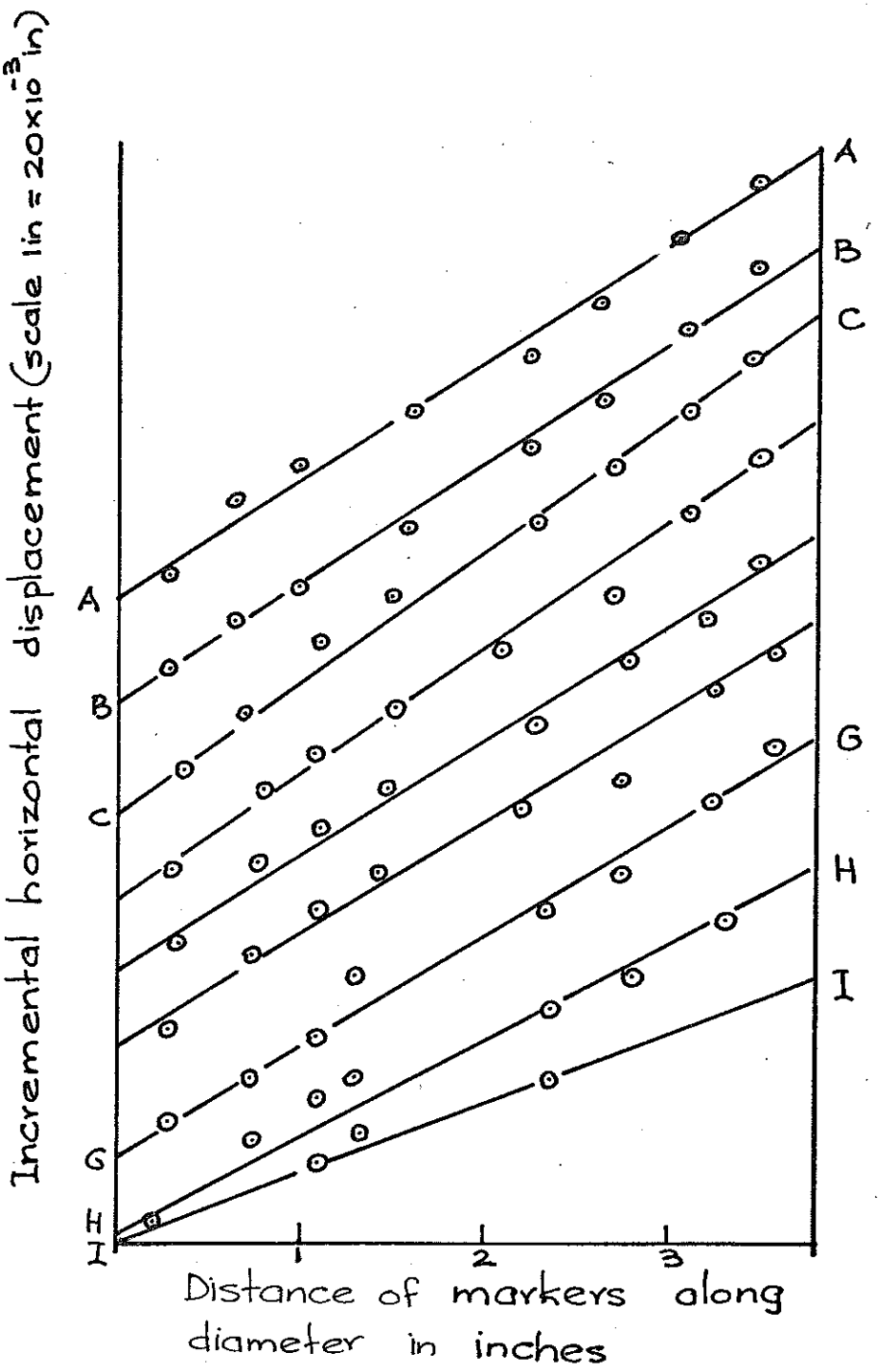

Fig. 3.20.(b) Incremental horizontal displacement of lead markers plotted against their distances along the diameter for nine horizontal rows in plane 2 of sample OC during isotropic swelling.

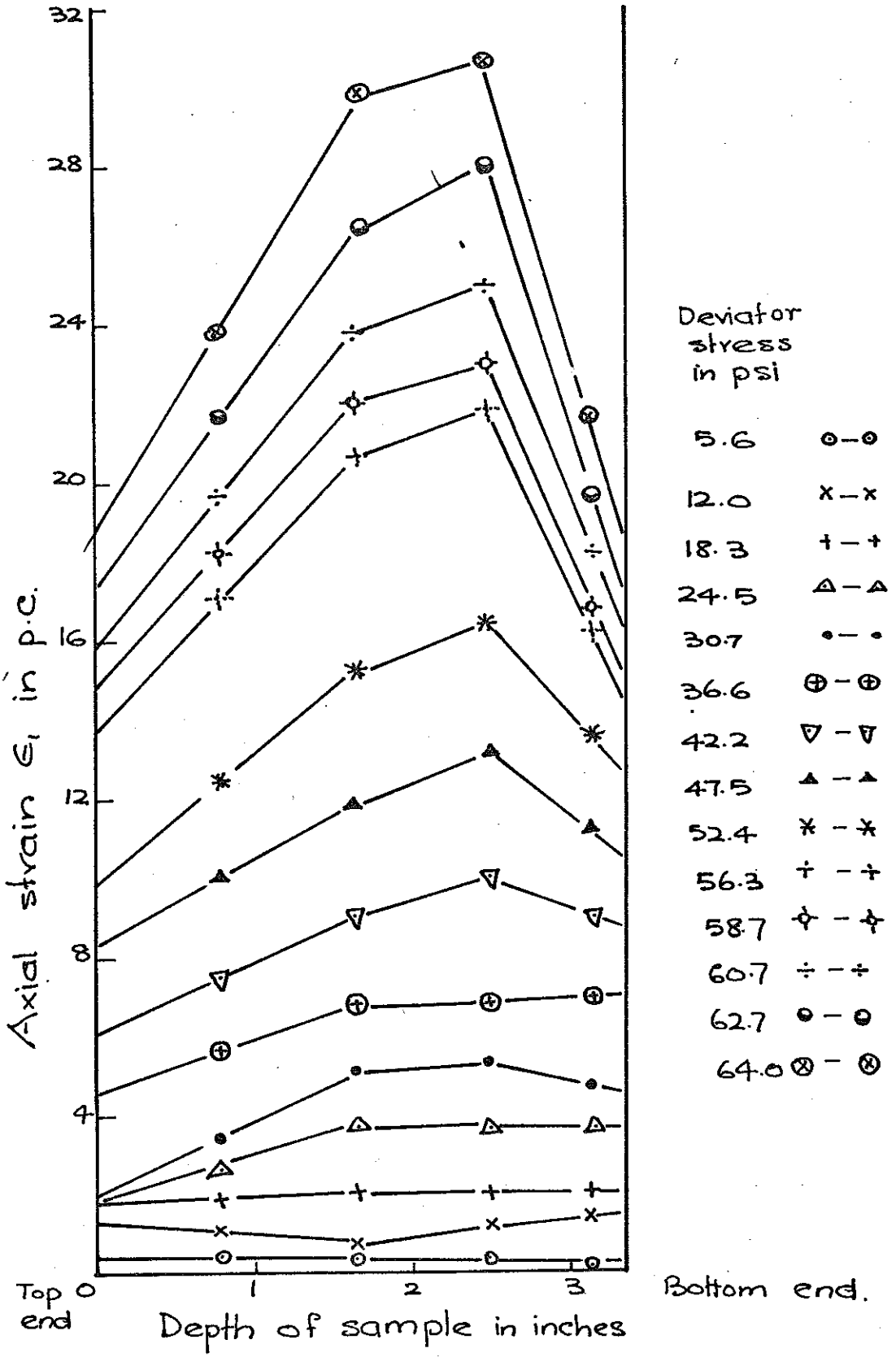

Fig. 3.21(a) Axial strain distribution in a 1.5 inch diameter sample contained between conventional frictional ends.
(Fully drained test T at 60 psi cell pressure)

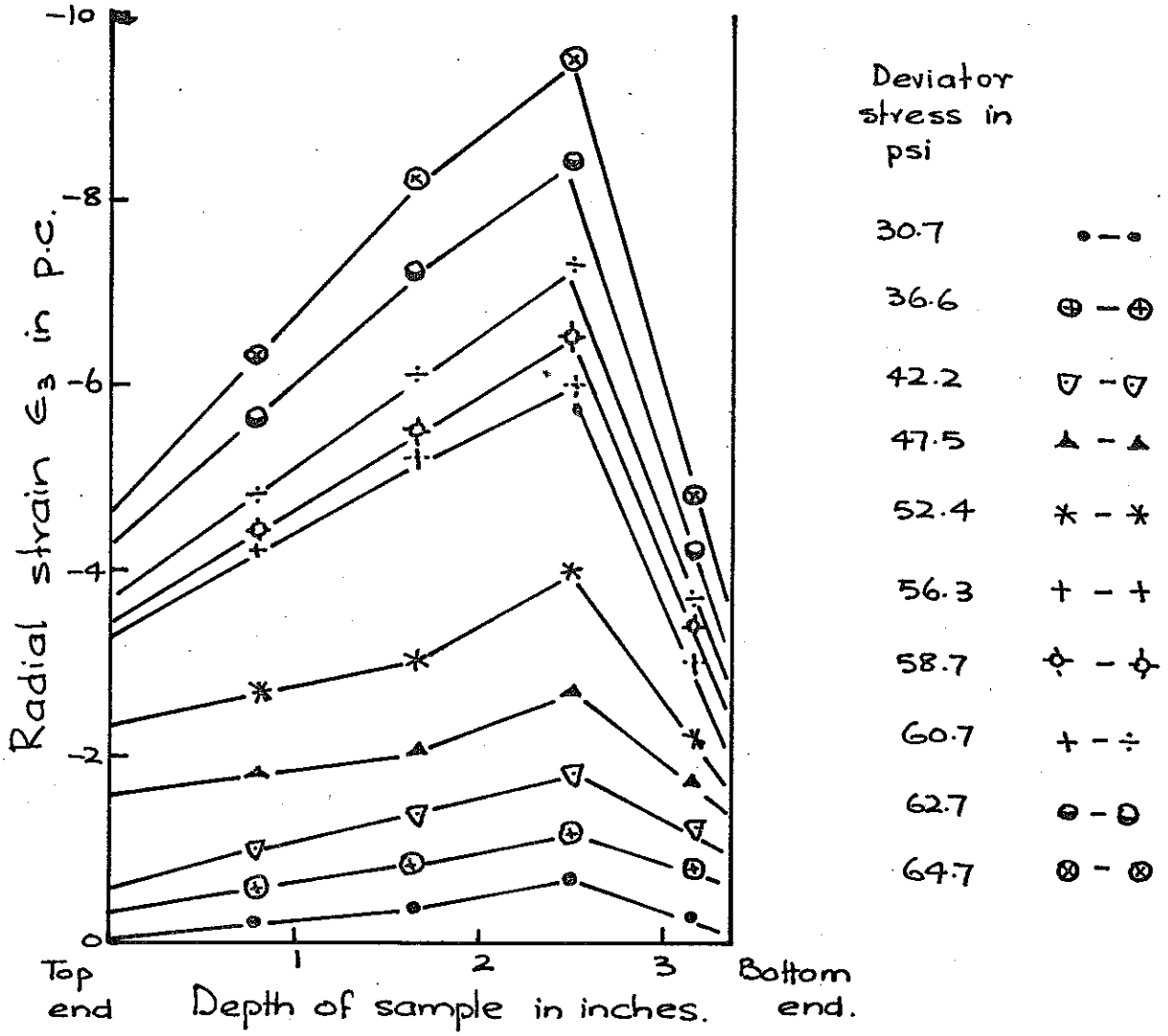

Fig. 3.21 (b) Radial strain distribution in 1.5 inch diameter sample contained between conventional frictional ends.

(Fully drained test T at 60 psi cell-pressure)

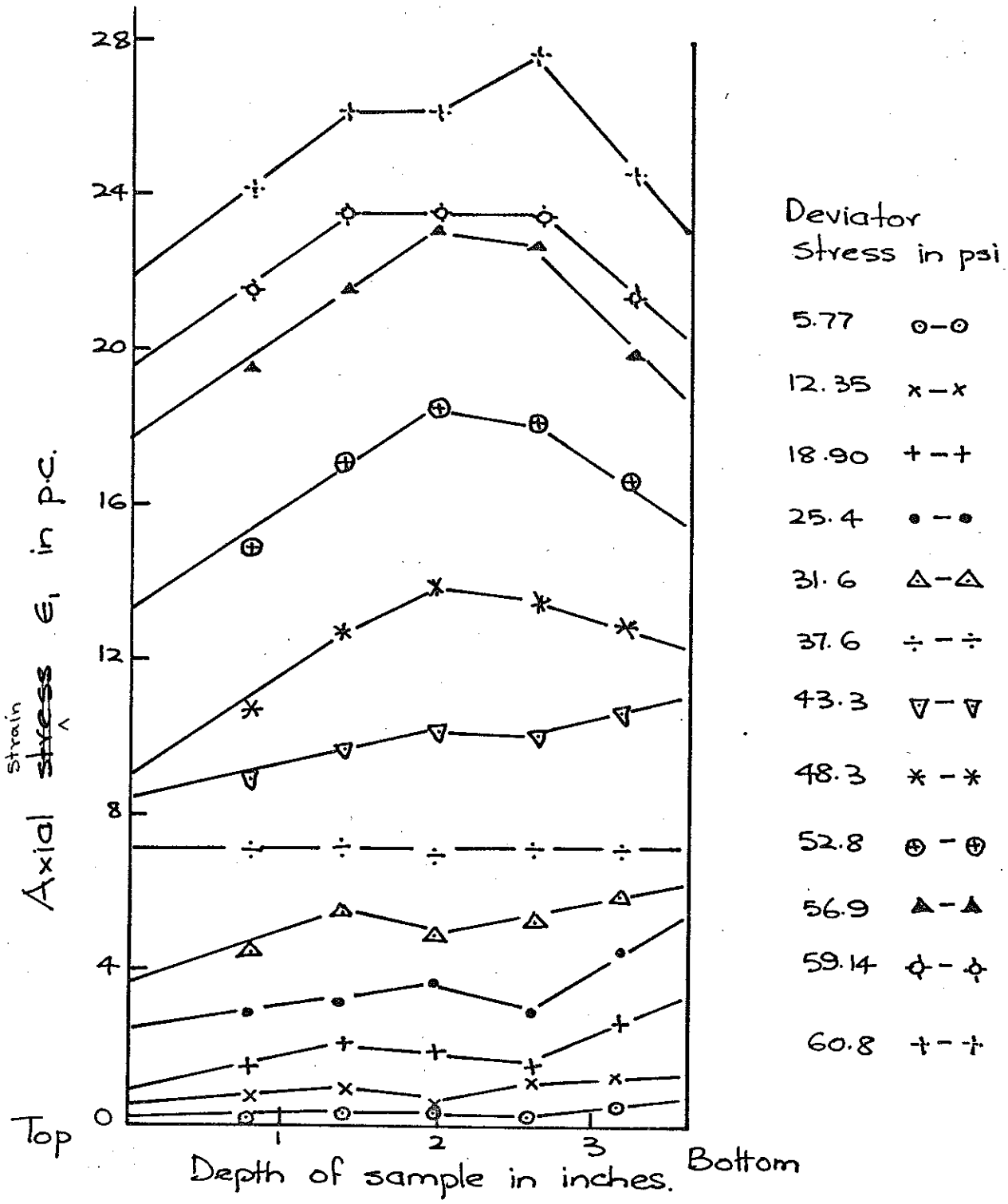

Fig. 3.22 (a) Axial strain distribution in a 1.5 inch diameter sample contained between conventional lubricated ends.

(Fully drained test R at 60 psi cell pressure)

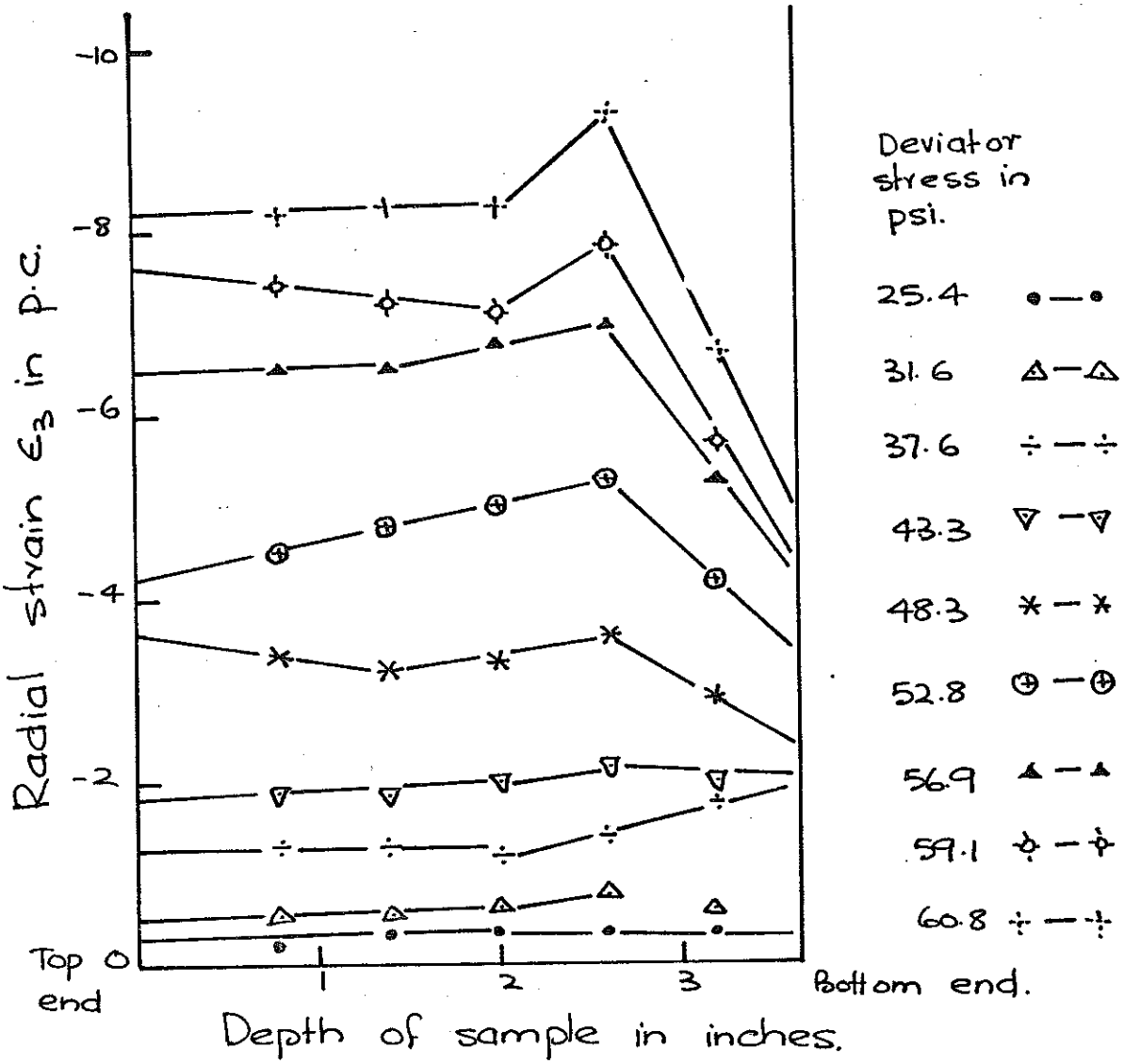

3.22 (b). Radial strain distribution in a 1.5 inch diameter sample contained between conventional lubricated ends.

(Fully drained test at 60 psi cell pressure)

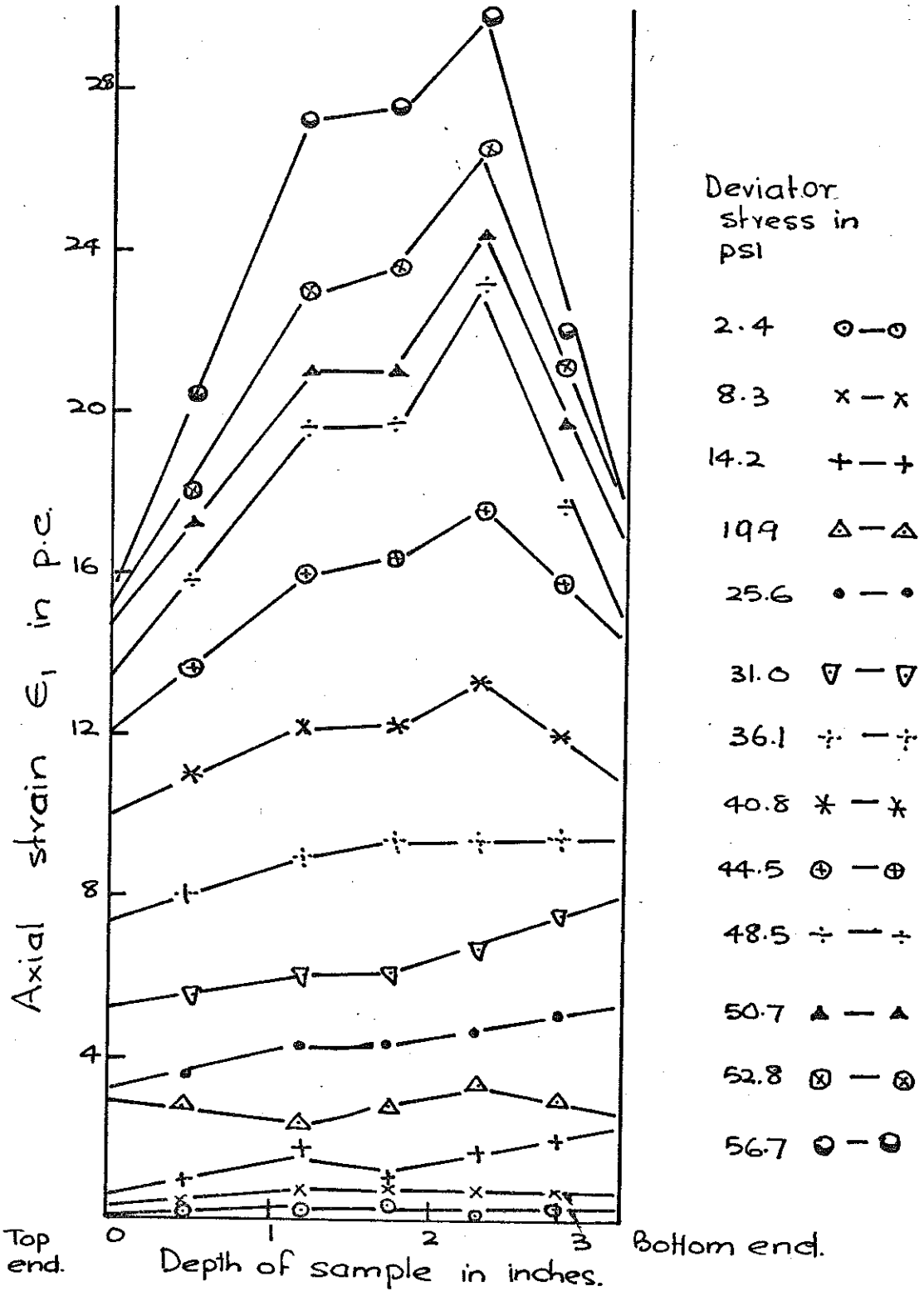

Fig. 3.23 (a) Axial strain distribution in a 1.5 inch diameter sample contained between enlarged lubricated ends.

(Fully drained test Q at 60 psi cell pressure)

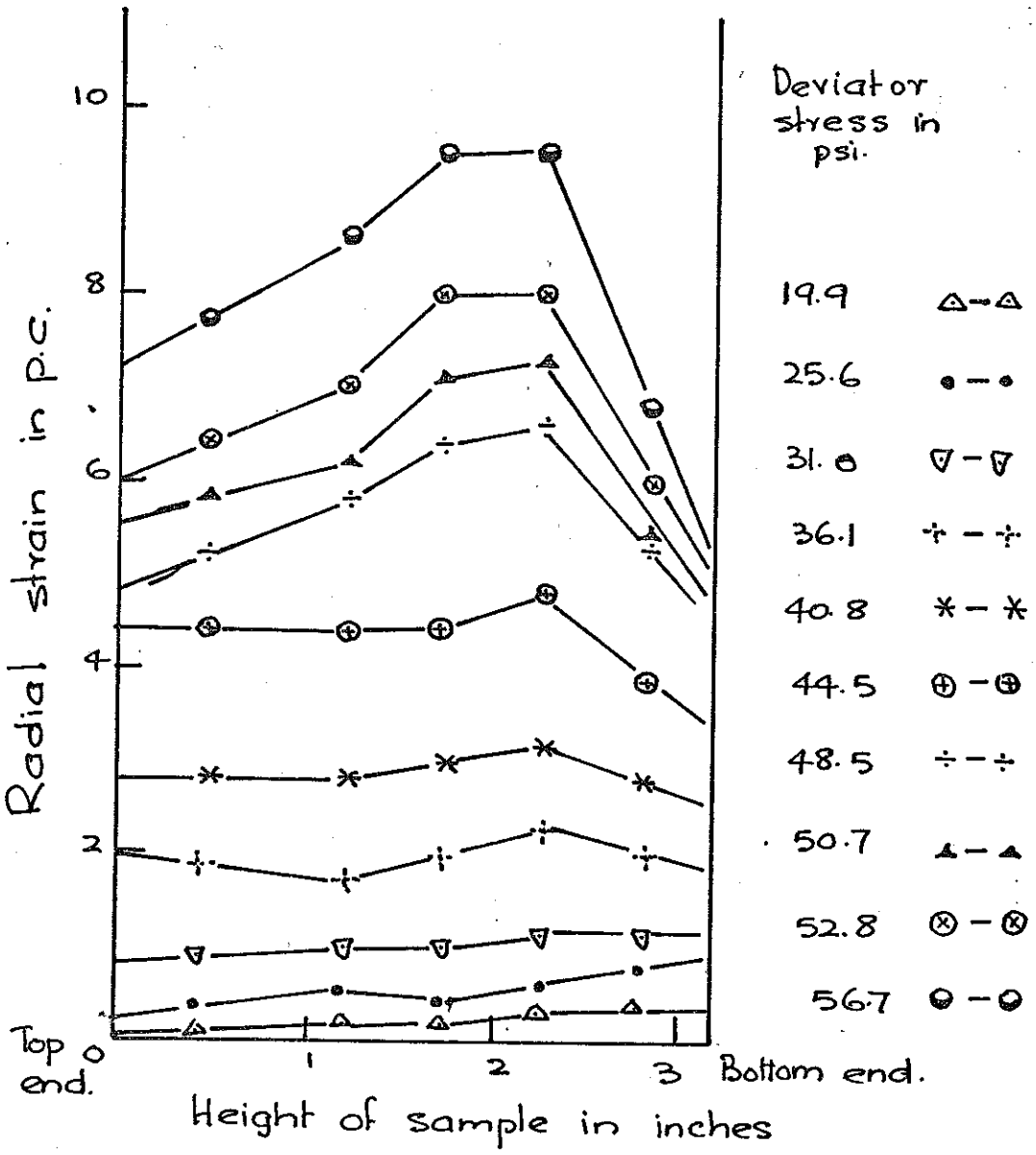

Fig. 3.23 (b). Radial strain distribution in a 1.5 inch diameter sample contained between enlarged lubricated ends.

(Fully drained test Q at 60 psi - cell pressure)

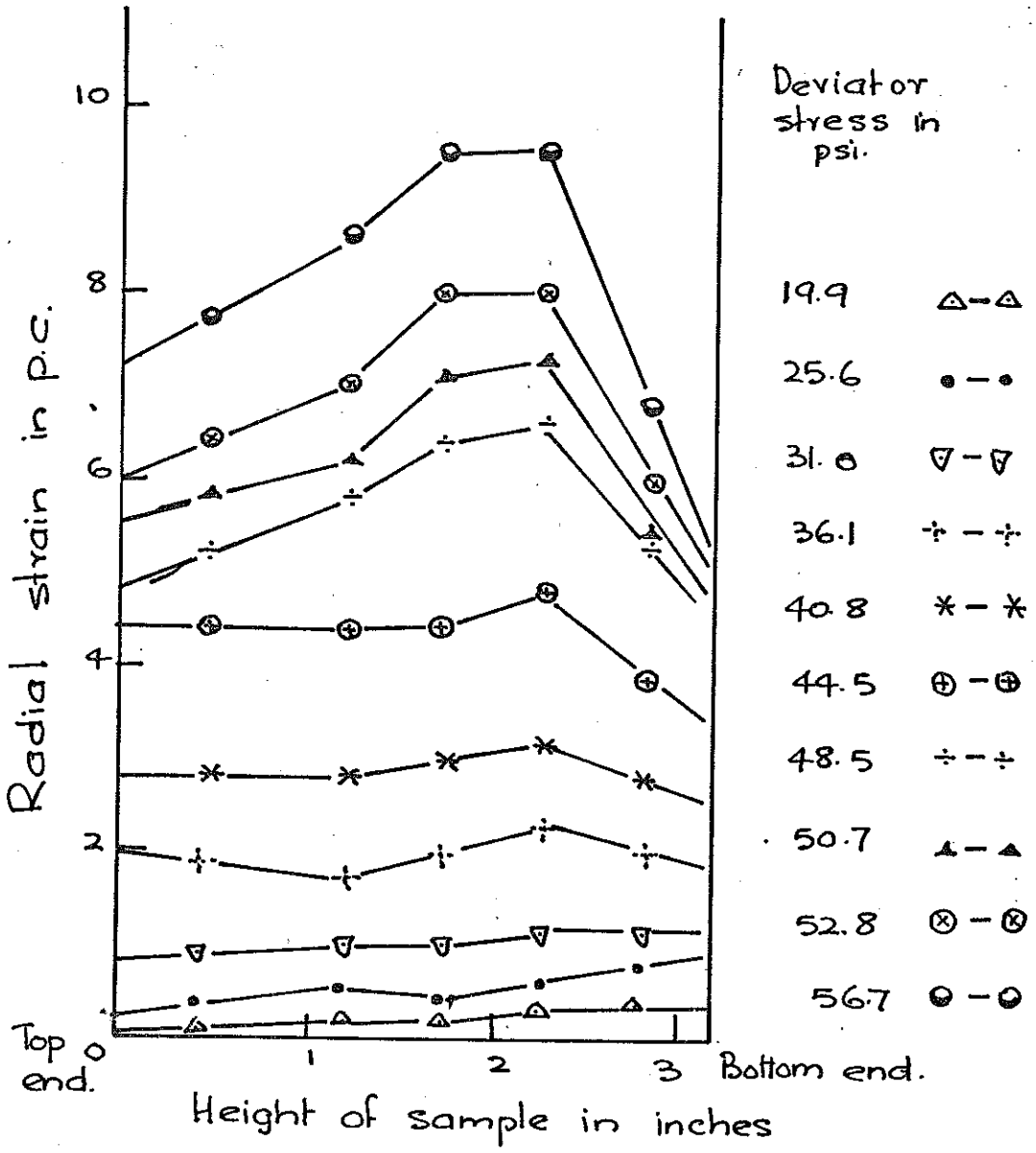

Fig. 3.23 (b). Radial strain distribution in a 1.5 inch diameter sample contained between enlarged lubricated ends.

(Fully drained test Q at 60 psi - cell pressure)

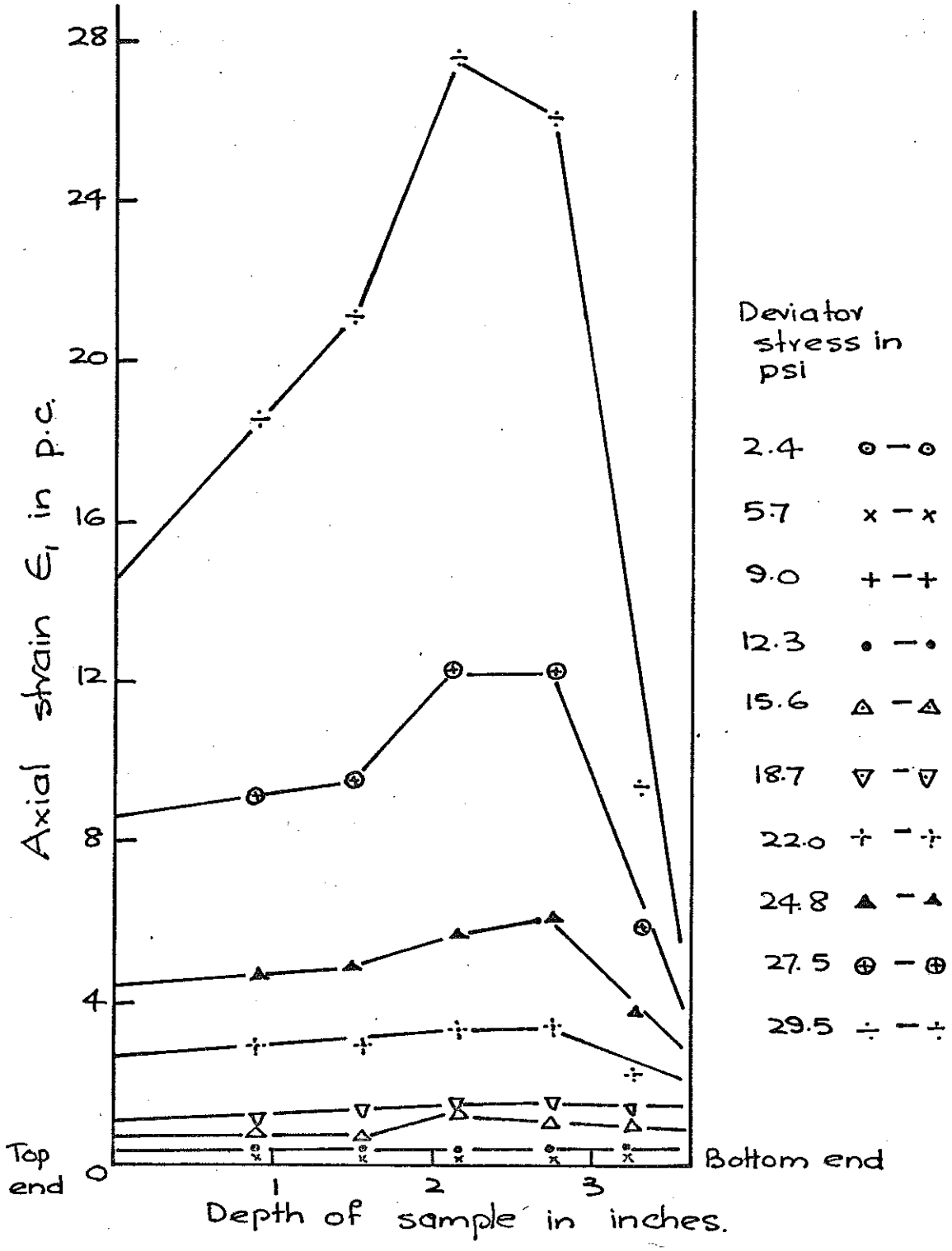

Fig.3.2.4 (a) Axial strain distribution in a 1.5 inch diameter sample contained between conventional frictional ends.

(Undrained test S at 60 psi cell pressure)

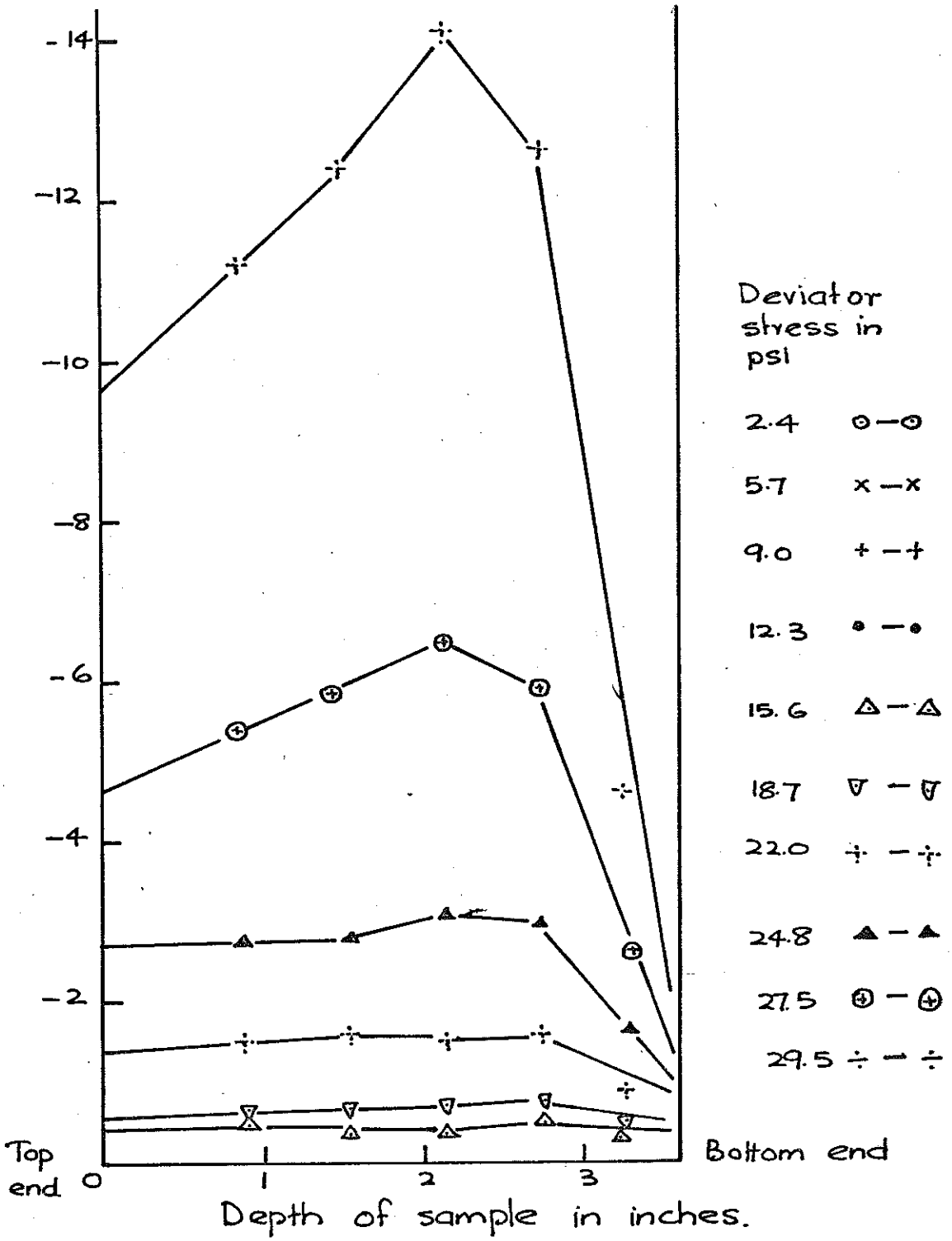

Fig. 3.24 (b). Radial strain distribution in a 1.5 inch diameter sample contained between conventional frictional ends.

(Undrained test S at 60 psi cell pressure)

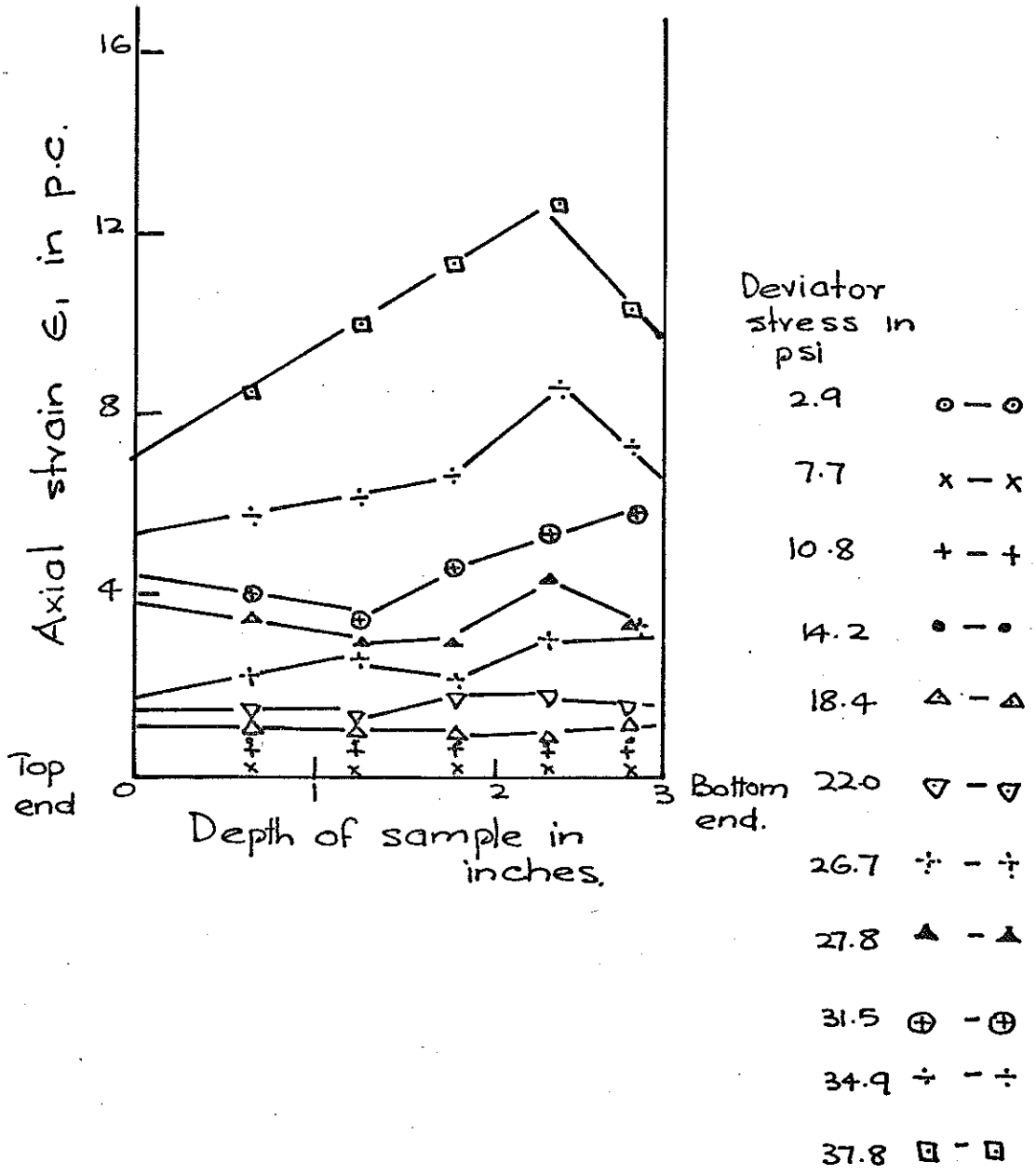

Fig. 3.25 (a) Axial strain distribution in a 1.5 inch diameter sample contained between enlarged lubricated ends.

(Undrained test U at 60 psi cell-pressure)

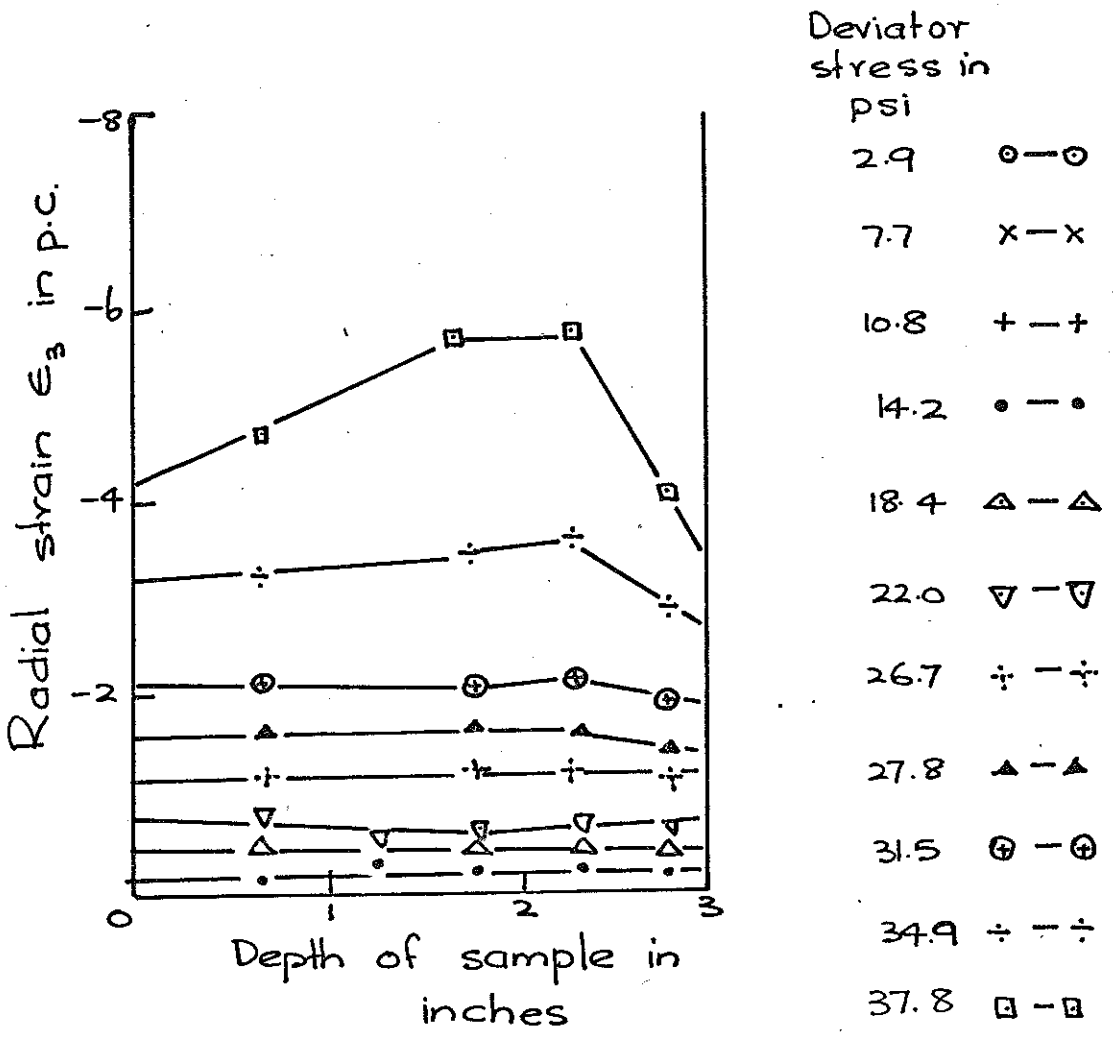

Fig. 3.25 (b). Radial strain distribution in a sample contained between enlarged lubricated ends.

(Undrained test U at 60 psi cell pressure)

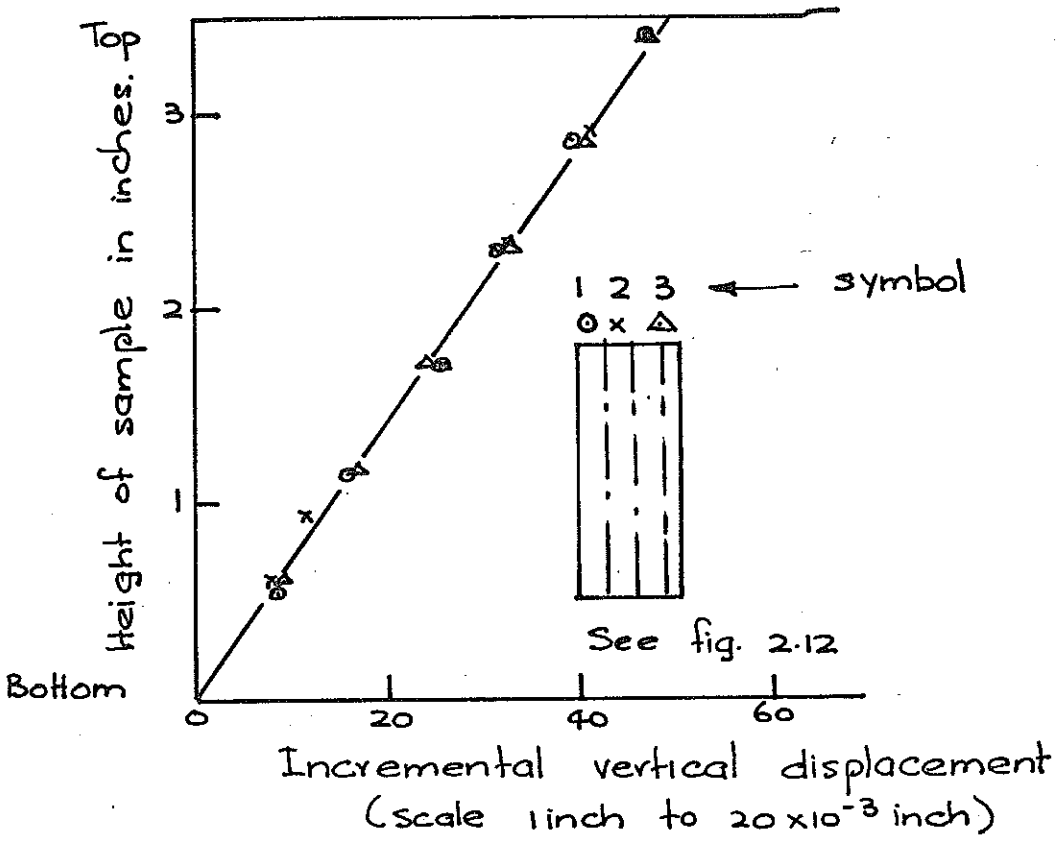

3.26 (a) Incremental vertical displacement - pattern at $\eta = 0.28$ and $\Delta\eta = 0.08$

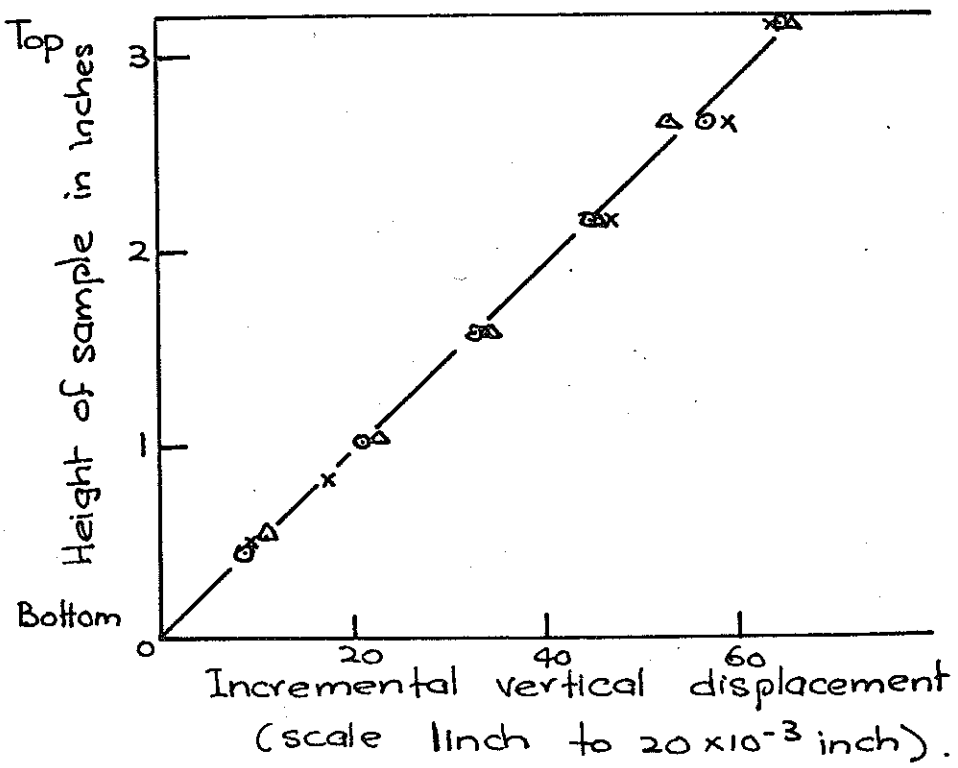

3.26 (b). Incremental Vertical displacement pattern at $\eta = 0.44$, $\Delta\eta = 0.07$

(See overleaf)

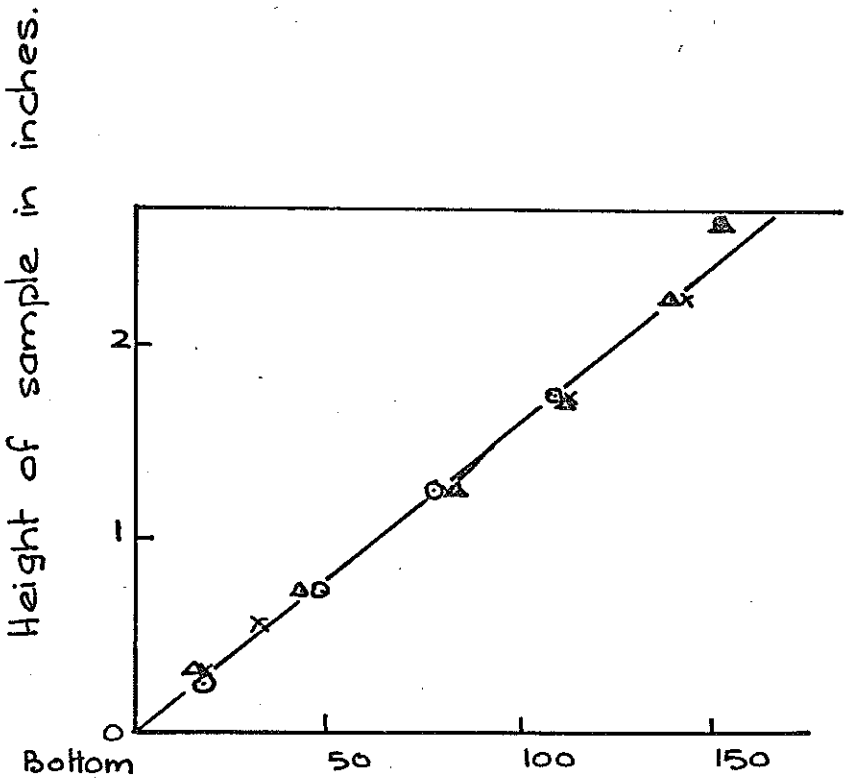

3.26 (c) Incremental vertical displacement pattern at $\eta = 0.62$ and $\Delta\eta = 0.06$.

3.26 (a-c) Incremental vertical displacement patterns in plane 1 of the normally consolidated sample AB for three increments of stresses during a fully drained test.

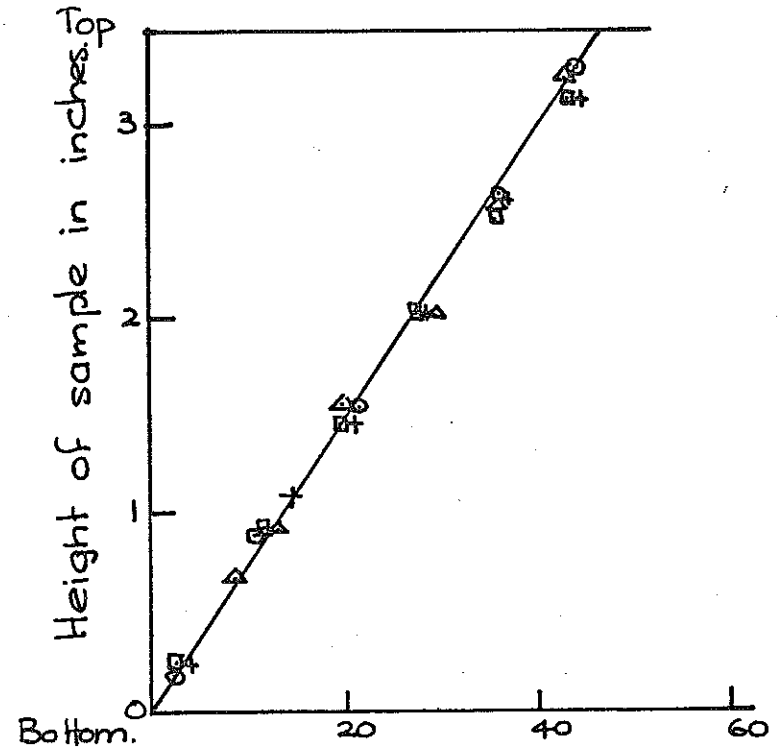

3.27 (a) Incremental vertical displacement.
(scale 1 inch to 20×10^{-3} inch)

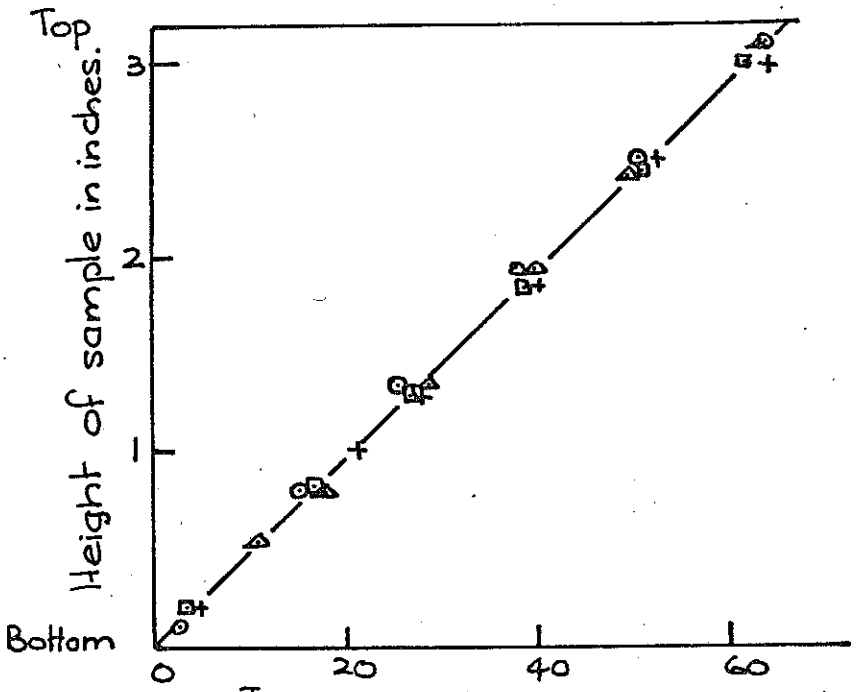

Incremental vertical displacement
(scale 1 inch to 20×10^{-3} inch)

3.27 (b). Incremental vertical displacement pattern at $\eta = 0.44$ and $\Delta\eta = 0.07$

(See overleaf)

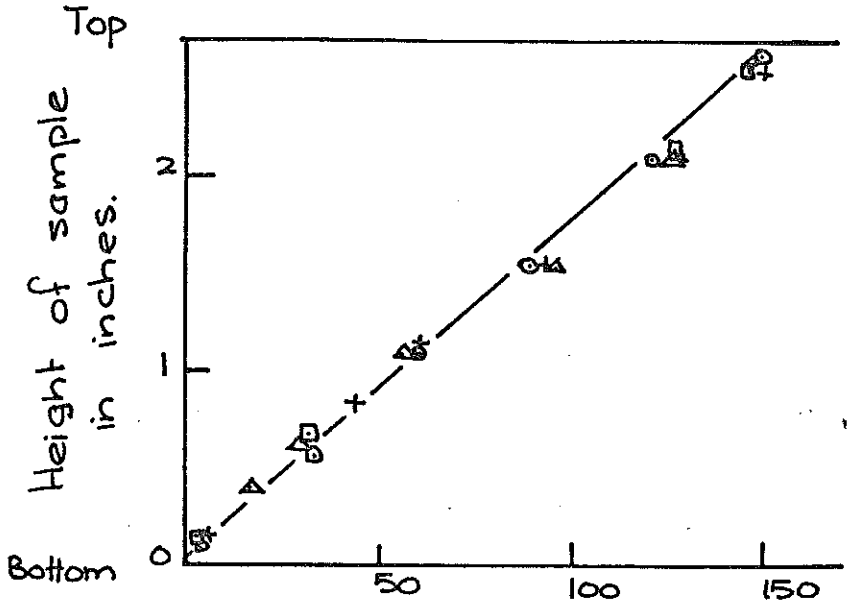

3.27 (c) Incremental vertical displacement pattern at $\eta = 0.62$ and $\Delta\eta = 0.06$.

Fig. 3.27 (a-c) Incremental vertical displacement patterns in plane 1 and plane 2 of the normally consolidated sample AB for three increments of stresses during a fully drained test.

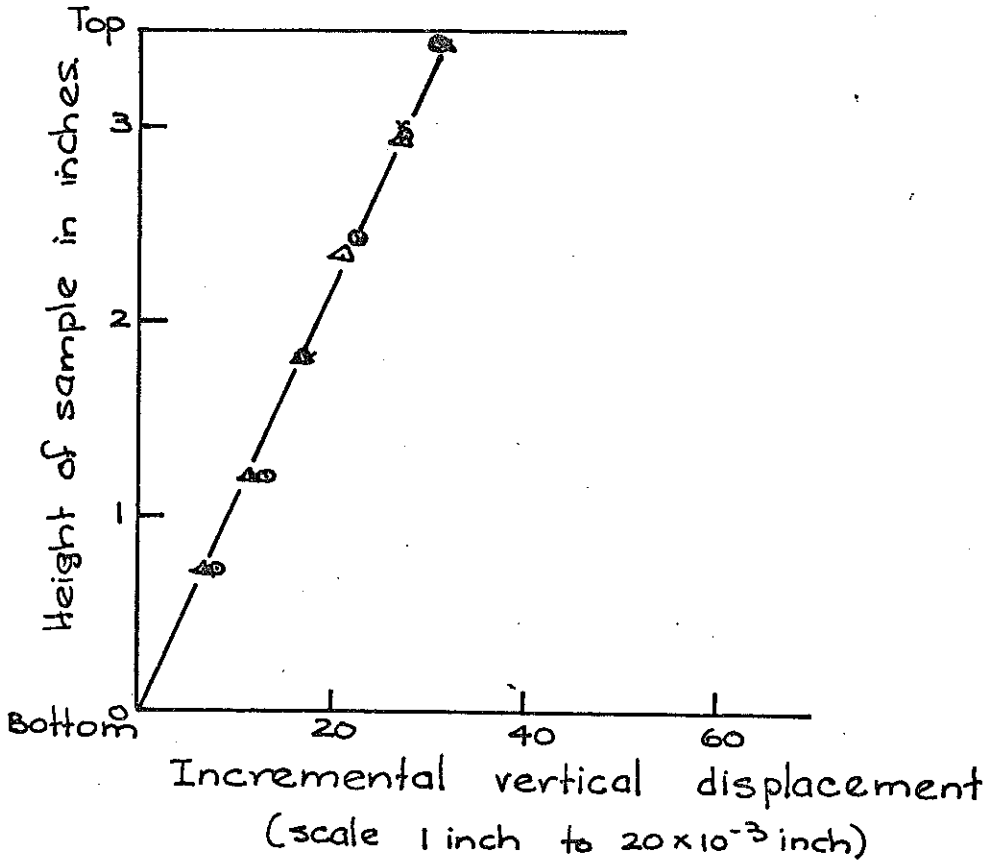

Fig. 3.28(a) Incremental vertical displacement pattern at $\eta = 0$ and $\Delta\eta = 0.18$.

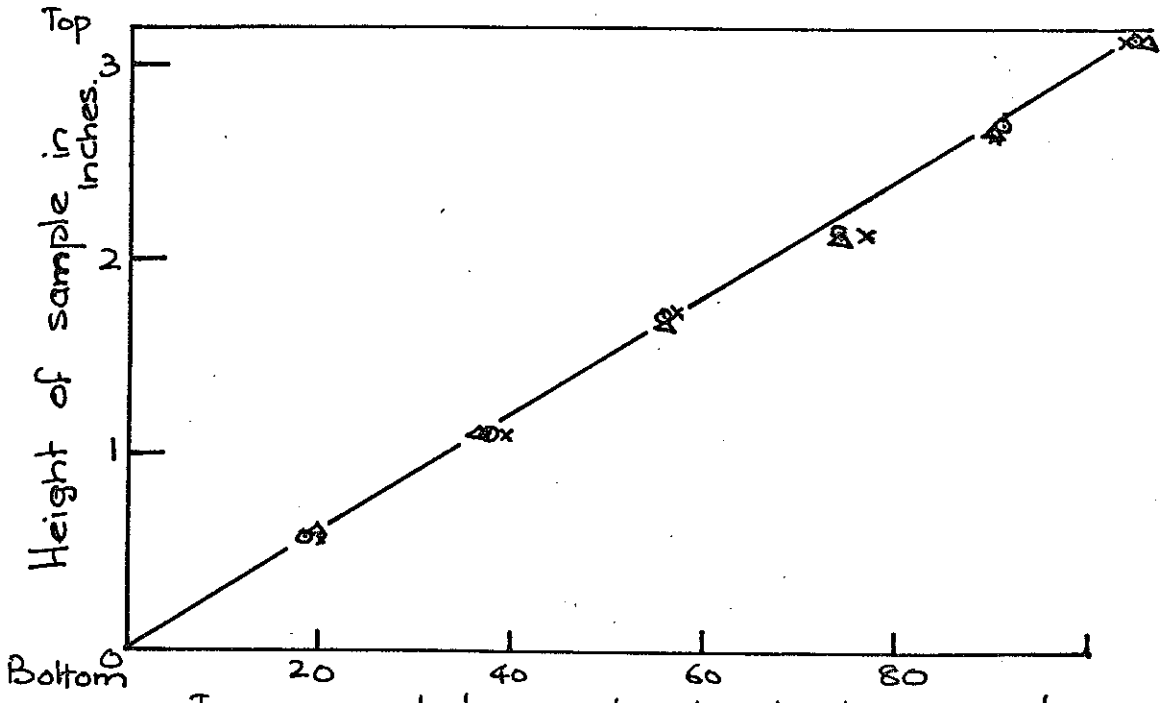

Fig. 3.28 (b). Incremental vertical displacement pattern at $\eta = 0.29$ and $\Delta\eta = 0.09$.

(See overleaf)

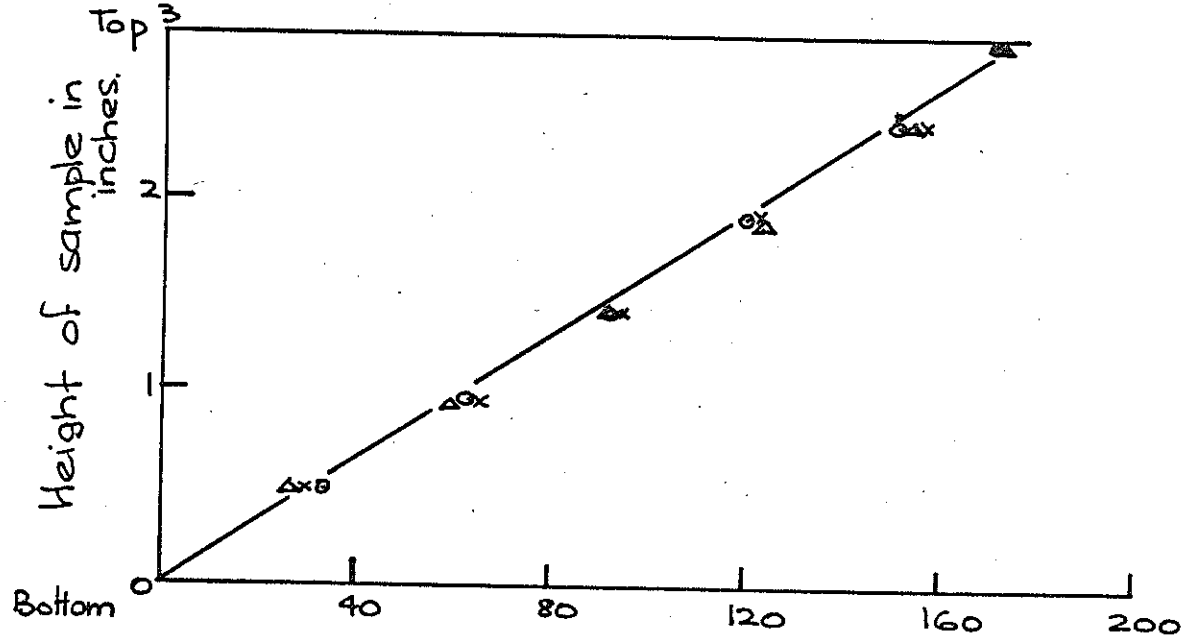

Fig 3.28 (c). Incremental vertical displacement pattern at $\eta = 0.48$ and $\Delta\eta = 0.11$.

Fig. 3.28 (a-c) Incremental vertical displacement patterns of lead markers in plane 1 of normally consolidated sample AX. (sheared from 60 psi with applied stress path of slope 1.5)

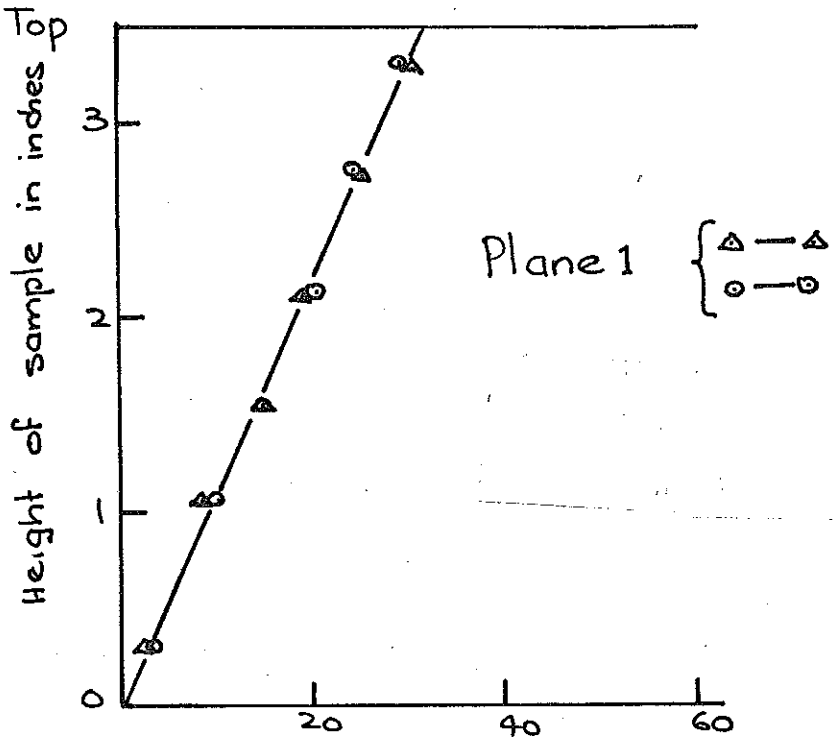

Incremental vertical displacement
(scale 1 inch to 20×10^{-3} inch).

3.29 (a) Incremental vertical displacement pattern at $\eta = 0$ and $\Delta\eta = 0.18$.

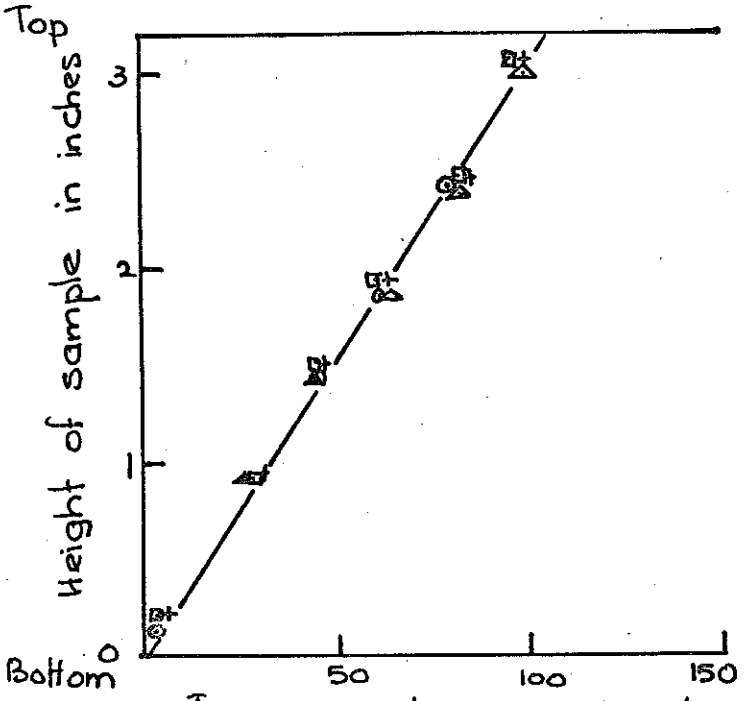

Incremental vertical displacement.
(scale 1 inch to 50×10^{-3} inch)

3.29 (b): Incremental vertical displacement pattern at $\eta = 0.29$ and $\Delta\eta = 0.09$

(See overleaf)

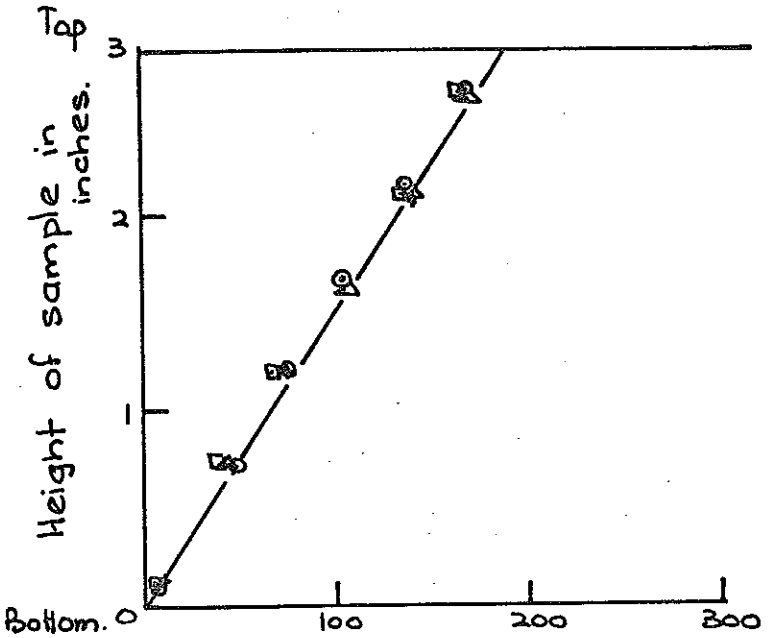

3.29(c). Incremental vertical displacement pattern at $\eta = 0.48$ and $\Delta\eta = 0.11$

Fig. 3.29 (a-c): Incremental vertical displacement patterns of lead markers in planes 1 and 2 of normally - consolidated sample AX

(sheared from 60psi cell pressure with applied stress path of slope 1.5)

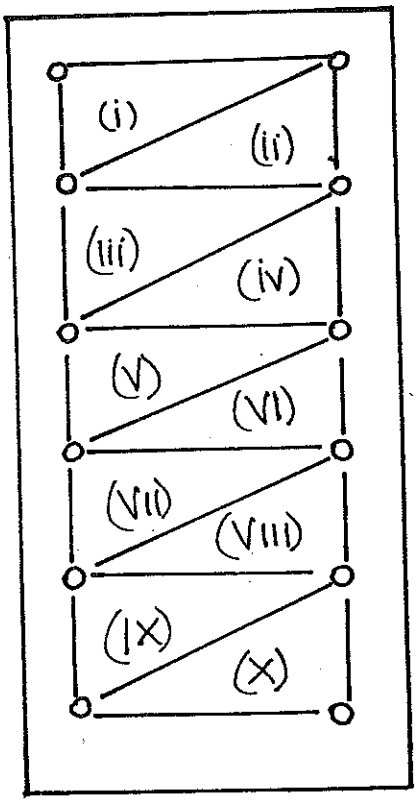

Fig. 3.30 Illustration of triangular elements in sample AB for computation of strains.

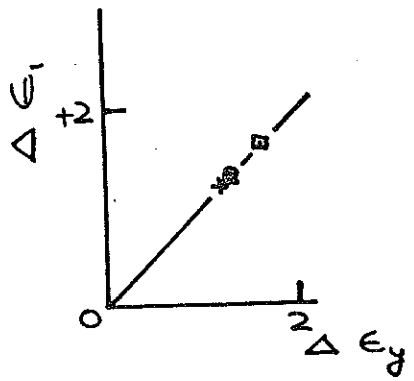

Odd numbered triangles Fig. 3.30

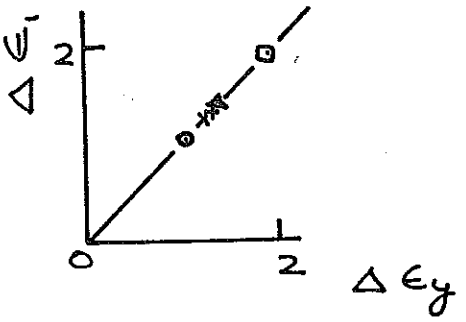

Even numbered triangles Fig. 3.30

(a) Incremental axial strain $\Delta\epsilon_y$ (Sirwan) and $\Delta\epsilon$ (author)

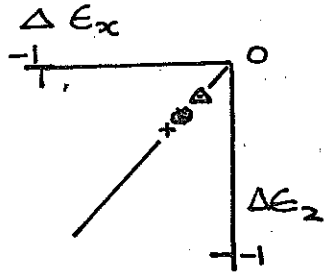

Odd numbered triangles

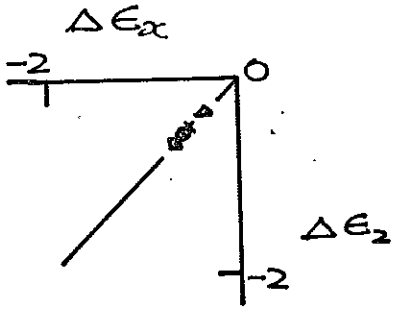

Even numbered triangles.

(b) Incremental radial strain $\Delta\epsilon_x$ (Sirwan) and $\Delta\epsilon_2$ (author)

Fig. 3.31. Comparison of incremental axial and radial strains Sirwan's method ($\Delta\epsilon_y$, $\Delta\epsilon_x$) and author's method ($\Delta\epsilon_1$, $\Delta\epsilon_2$)

($\eta = 0.28$ and $\Delta\eta = 0.08$.)

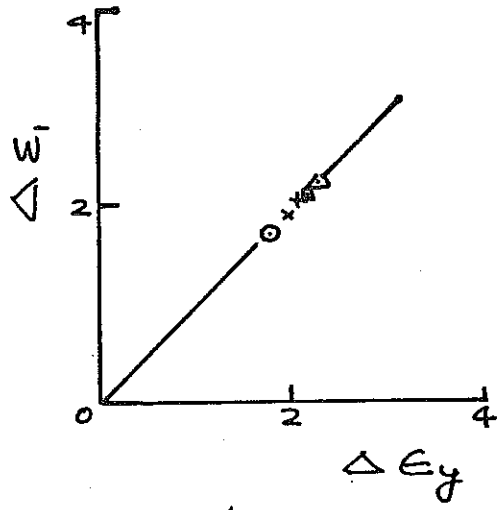

Odd numbered triangles in Fig. 3.30

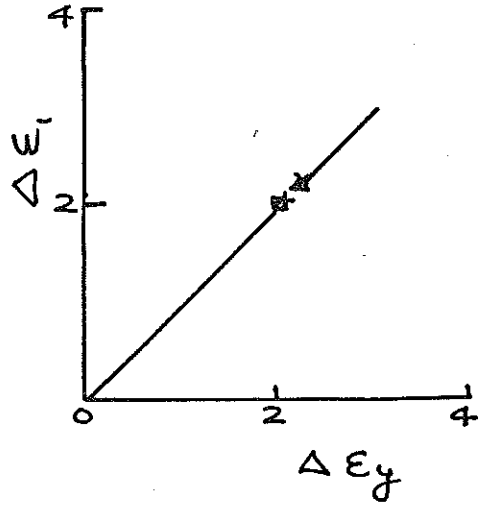

Even numbered triangles in Fig. 3.30

(a) Incremental axial strain $\Delta \varepsilon_y$ (Sirwan) and $\Delta \varepsilon_1$ (Author)

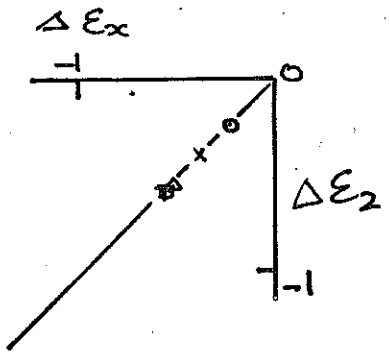

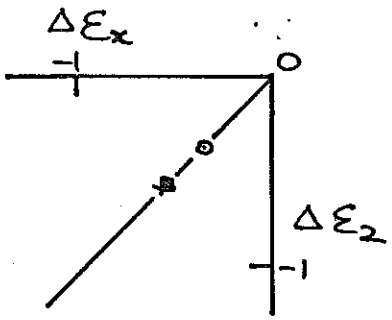

(b) Incremental radial strain $\Delta \varepsilon_x$ (Sirwan) and $\Delta \varepsilon_2$ (Author)

Fig. 3.32(a-b). Comparison of incremental axial and radial strains computed from Sirwan's method ($\Delta \varepsilon_y$, $\Delta \varepsilon_x$) and authors method ($\Delta \varepsilon_1$, $\Delta \varepsilon_2$)

($\eta = 0.44$ and $\Delta \eta = 0.07$.)

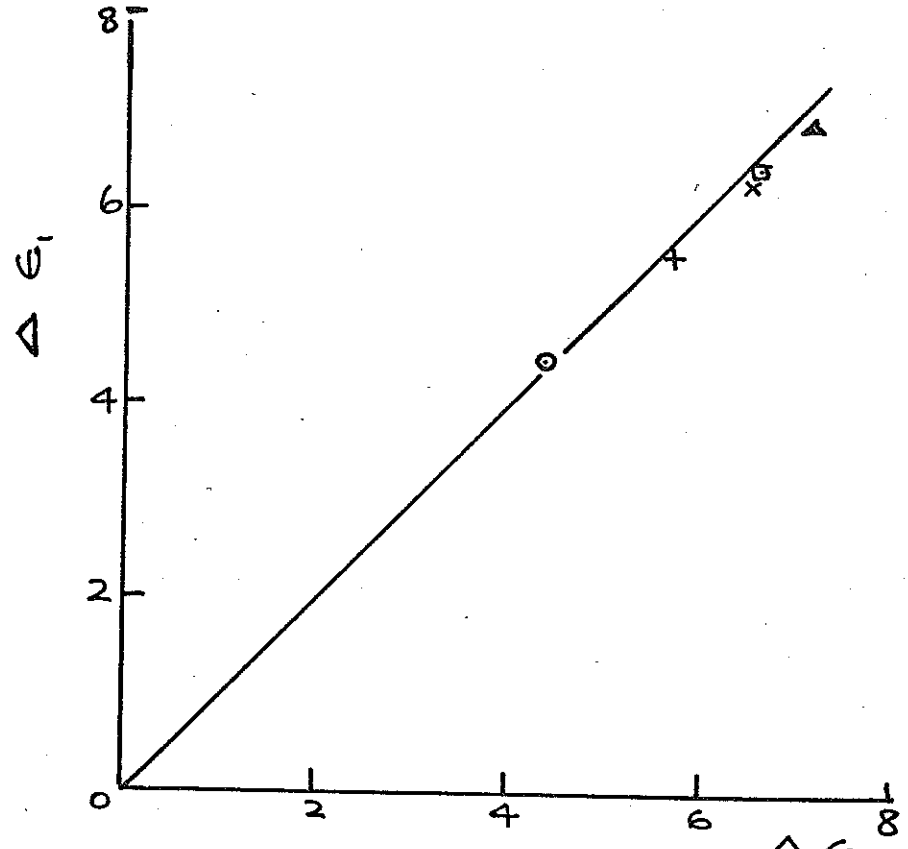

Odd numbered triangles.

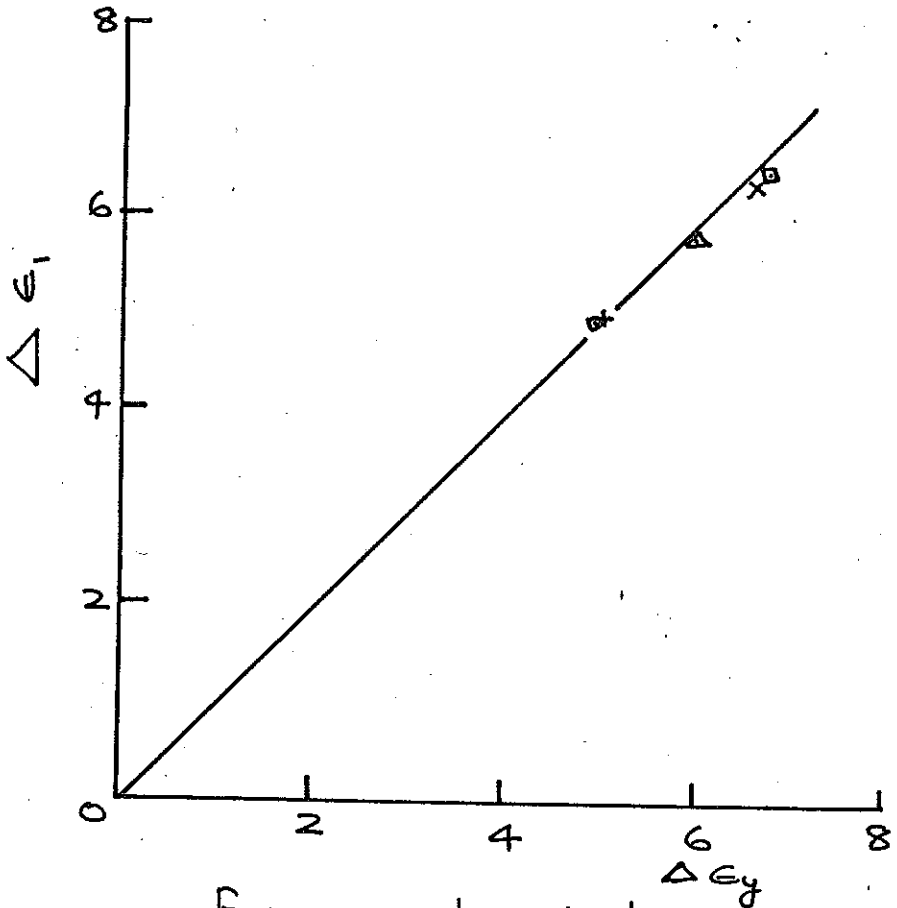

Even numbered triangles.

Fig. 3.33(a) Incremental axial strain $\Delta\epsilon_y$ (Sirwan) and $\Delta\epsilon_1$ (author)

(See overleaf.)

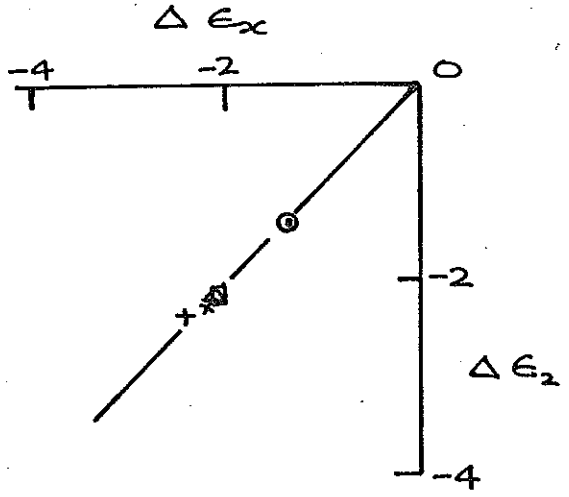

Odd numbered triangles in Fig. 3.30

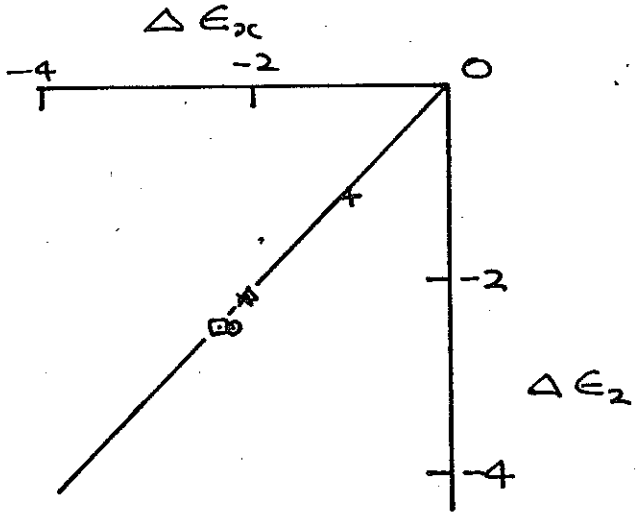

Even numbered triangles in Fig. 3.30.

(b) Incremental radial strain $\Delta\epsilon_x$ (Sirwan) and $\Delta\epsilon_2$ (author).

Fig. 3.33 (a-b) Comparison of incremental axial and radial strains, computed from Sirwan's method ($\Delta\epsilon_y, \Delta\epsilon_x$) and author's method. ($\gamma = 0.62$, $\Delta\gamma = 0.06$)

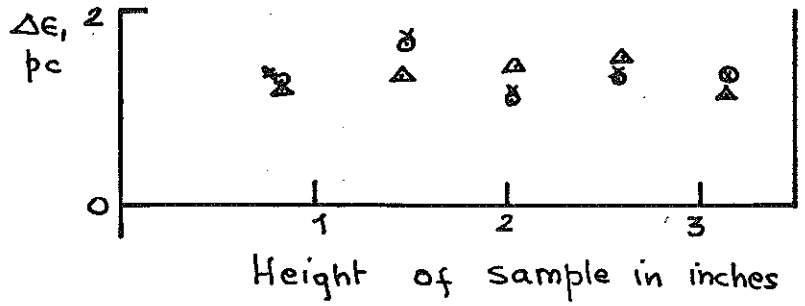

(ii) $\eta = 0.28$ $\Delta\eta = 0.08$

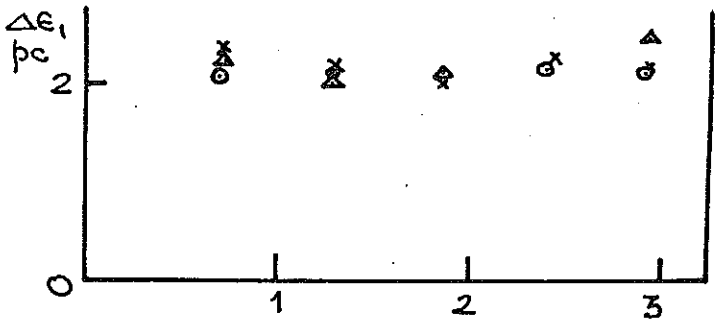

(iii) $\eta = 0.44$ $\Delta\eta = 0.07$

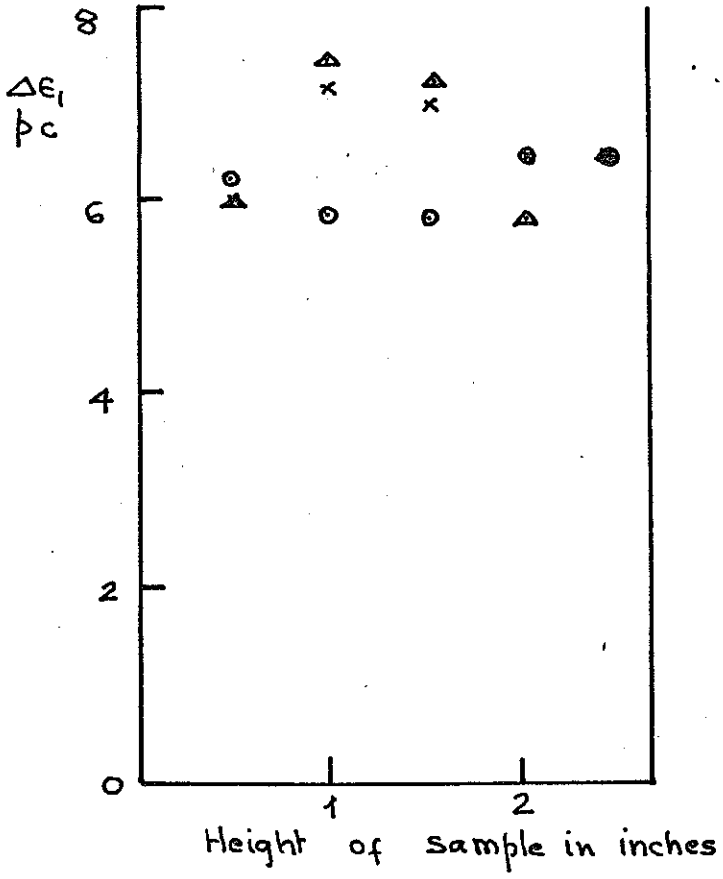

(iii) $\eta = 0.62$ $\Delta\eta = 0.06$

Fig. 3.34 Incremental axial strain distributions in the normally consolidated sample AB during a fully drained test with constant cell pressure.

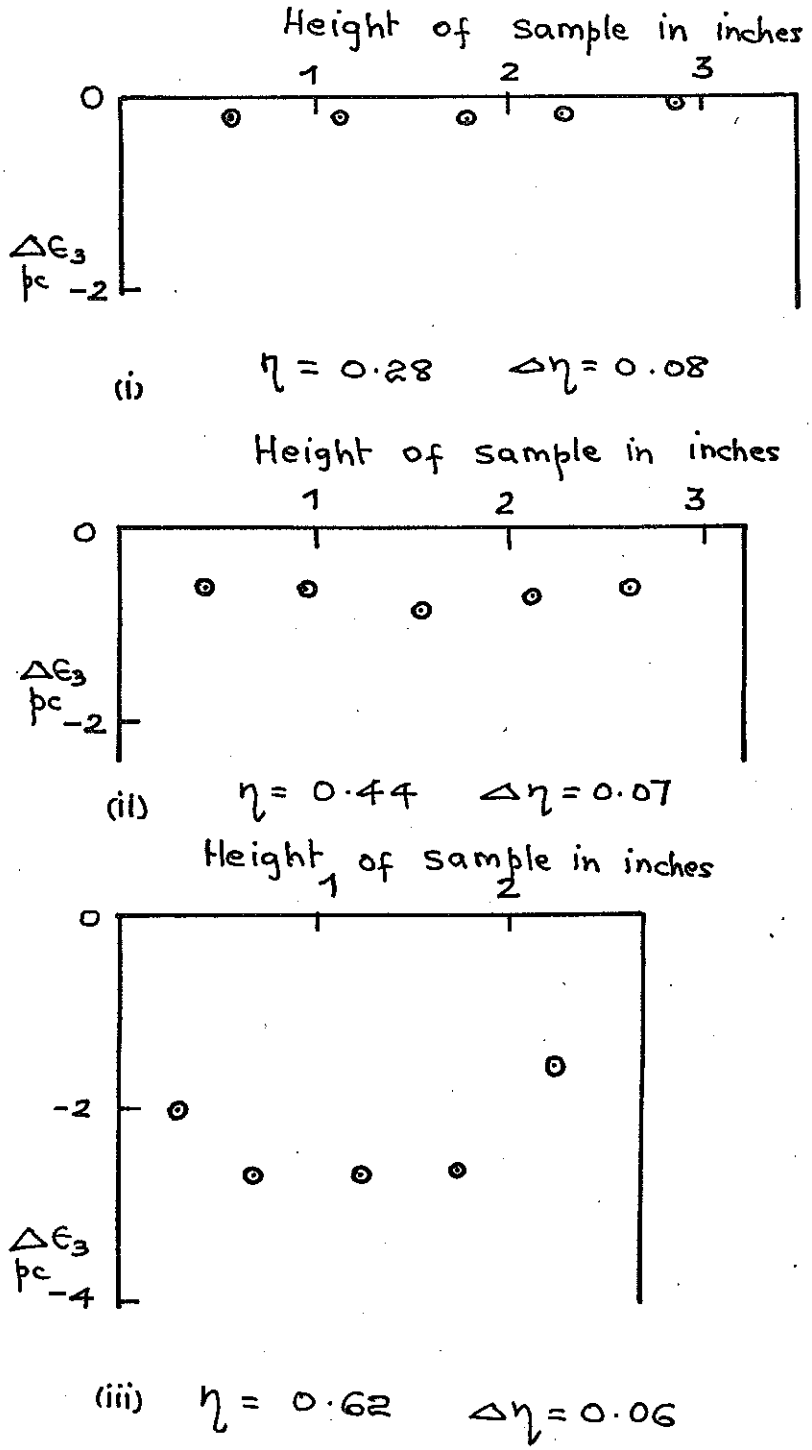

Fig. 3.35. Incremental radial strain distribution in the normally consolidated sample AB during a fully drained test with constant cell pressure.

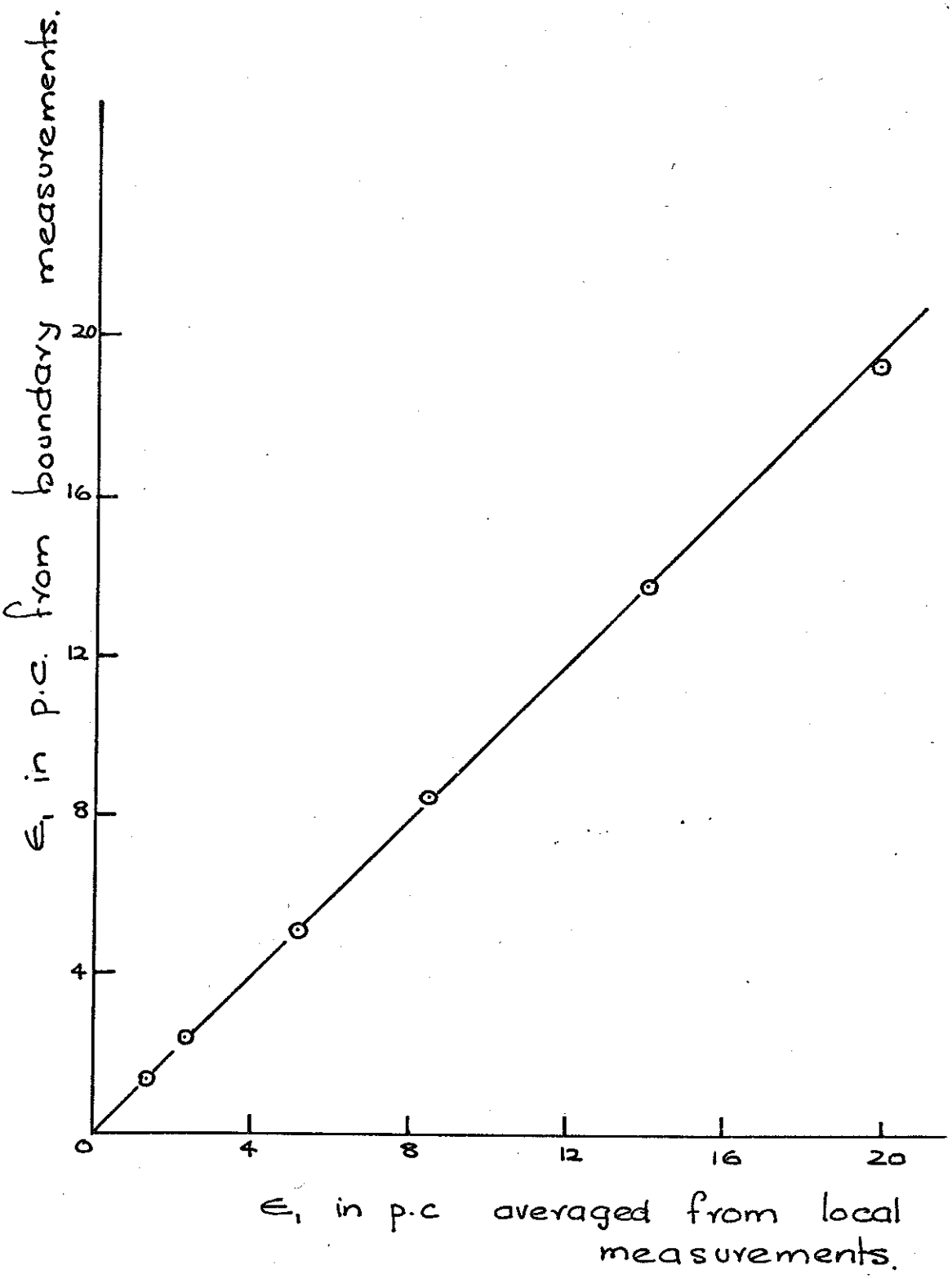

Fig33 6 (a) Comparison of the average axial strain from local measurements and the average axial strain from boundary measurements. in sample Ax

(applied stress path of slope 1·5 at 60 psi)

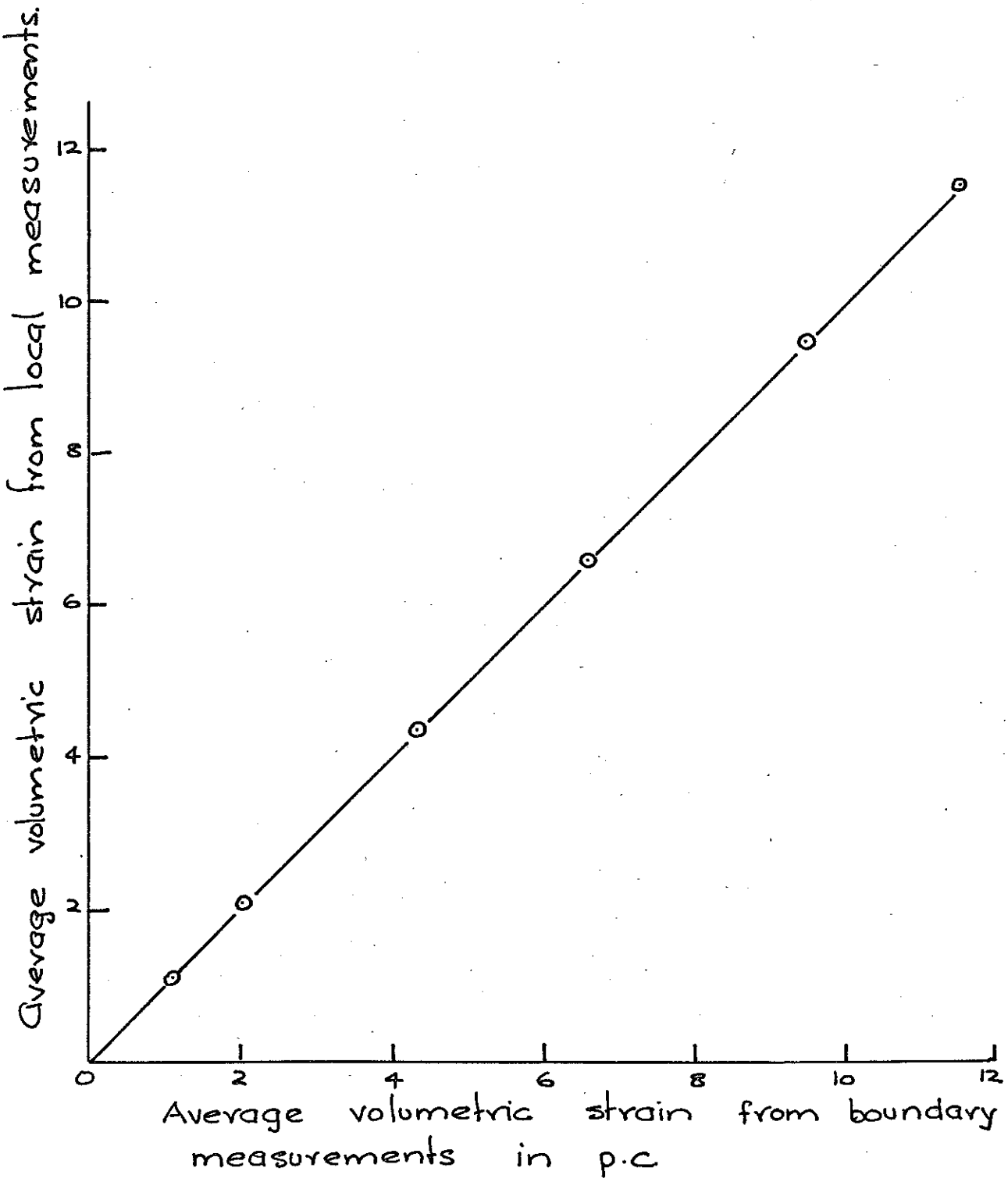

Fig. 3.36(b). Comparison of the volumetric strain from boundary measurements and the average volumetric strain from local measurements.
(sample Ax. applied stress path of slope 1.5 at 60 psi)

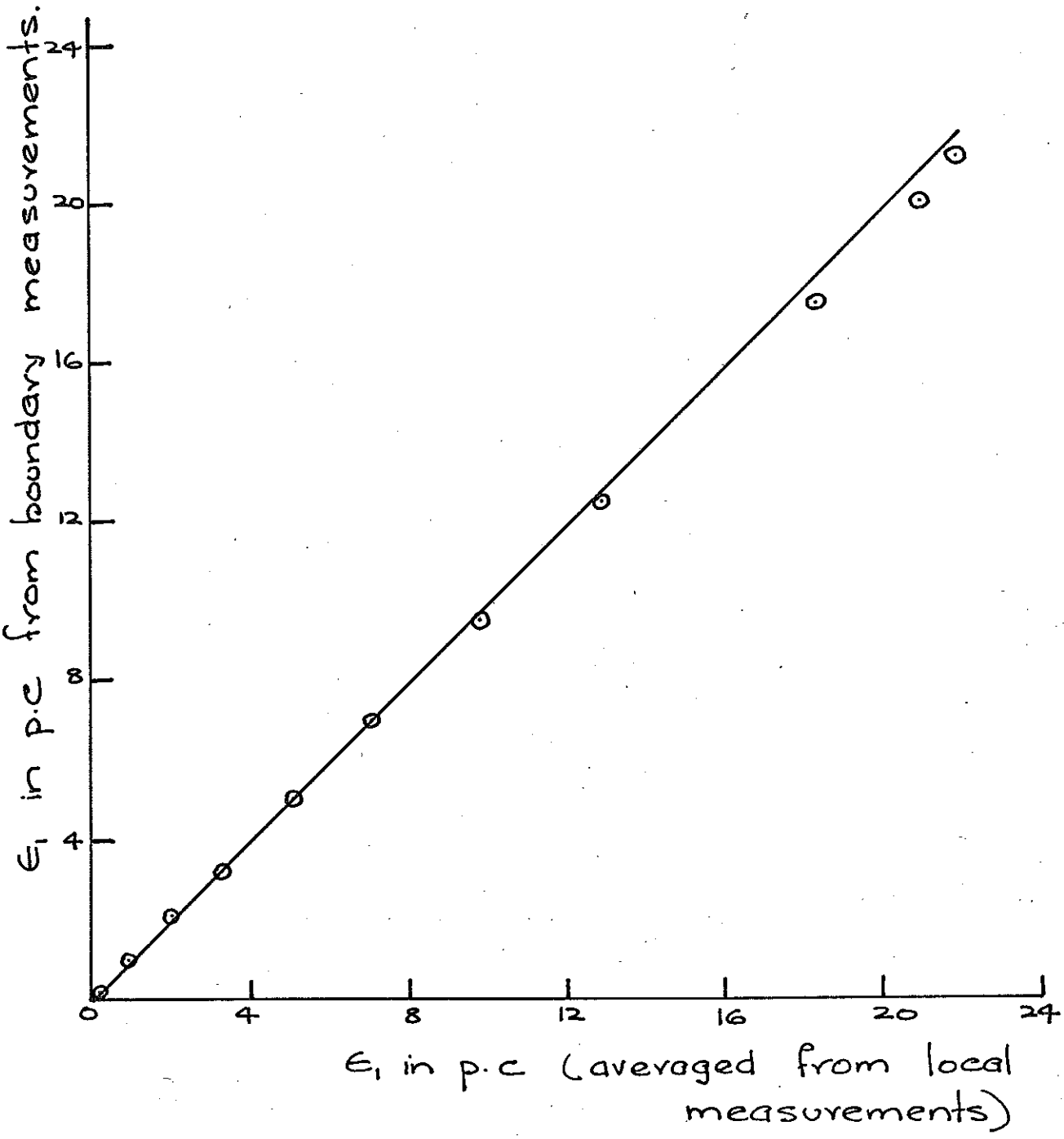

Fig. 3.37 (a) Comparison of average axial strain from boundary measurements and that from local measurements in sample AB.

(applied stress path of slope 3 from 60psi cell pressure)

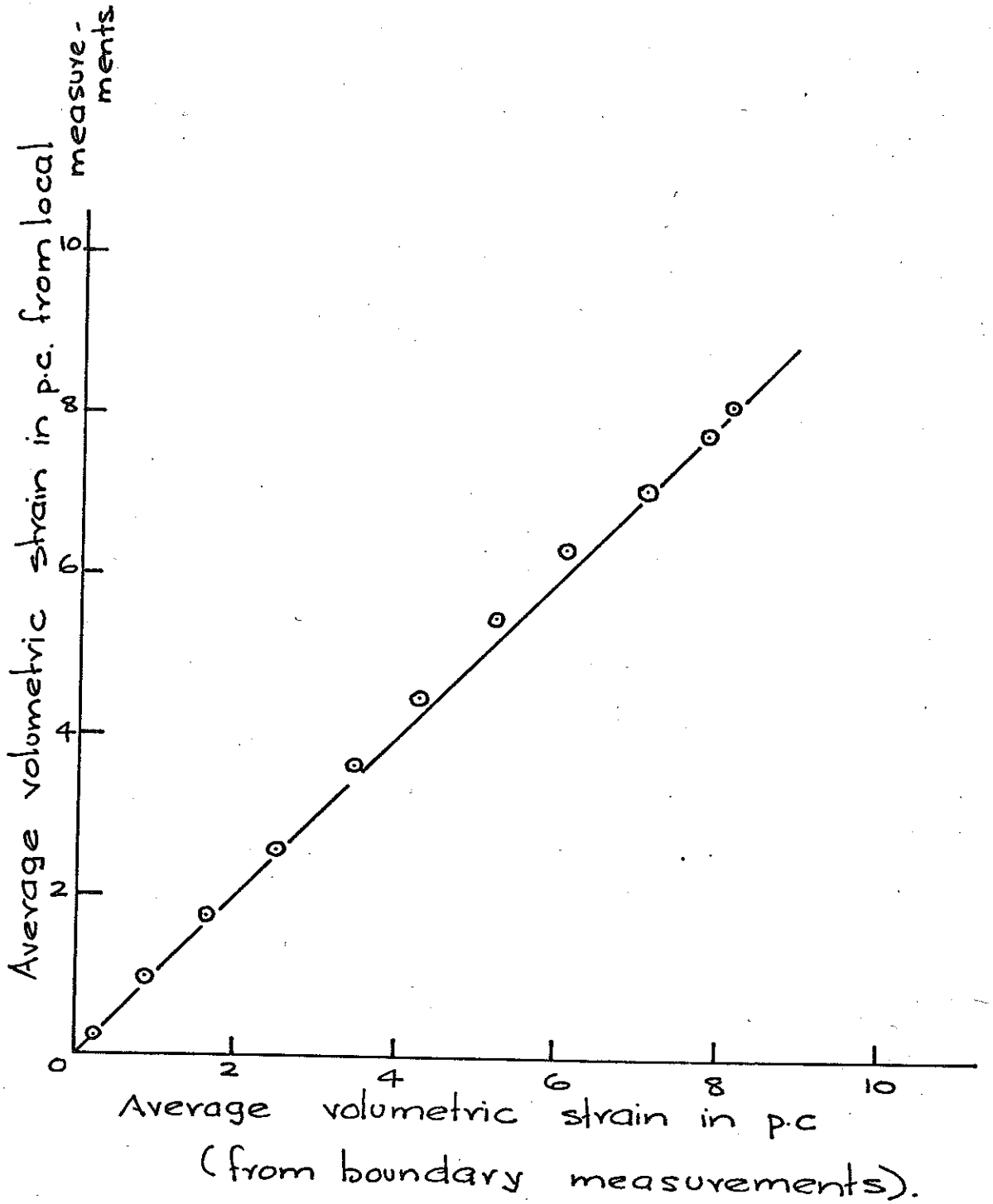

Fig. 3.37 (b) Comparison of volumetric strain from boundary measurements and average volumetric strain from local measurements in sample AB

(applied stress path of slope 3 at 60 psi cell pressure)